

## Catastrophic 1638 earthquakes in Calabria (southern Italy): New insights from paleoseismological investigation

Paolo Galli and Vittorio Bosi

Civil Protection Department, Seismic Survey of Italy, Rome, Italy

Received 14 December 2001; revised 6 June 2002; accepted 7 October 2002; published 3 January 2003.

[1] The reanalyses of all the primary historical sources of the catastrophic March–June 1638 Calabrian earthquakes permitted to split up the seismic sequence in different events that occurred in conterminous areas and to direct our geological surveys of the June shock inside the Sila massif (northern Calabria). We carried out paleoseismological analyses along the Lakes fault (LF), a previously unknown fault. LF (trending NW-SE) cuts the eastern sector of the Sila massif and dips southwestward, damming the drainage network that runs toward the Ionian Sea. We opened four trenches close to or inside some of the small marshes and ponds created by the footwall uplift, finding evidence of several displacement events, the last one being the June 1638 earthquake ( $M = 6.7$ ). The fault location fits with the historical description of a long fracture opened during the event, our trenching area being still named by the natives “the earthquake sag.” The young geomorphic expression of LF recalls that of the 1980 Irpinia fault, suggesting its relatively recent activation within the extensional regime characterizing the Calabrian arc.

Conversely, the northern continuation of LF (Cecita Lake fault), which we argue to be active too, is not associated to any historical earthquake of the Italian seismic catalogue, this fact evidencing a long, at least 1000 years, elapsed time. Our study permits (1) the relocation of the June 1638 earthquake inside the Sila massif, the epicenter being shifted with respect to the macroseismically derived one, (2) the revision of the whole 1638 sequence, (3) the discovery of the LF, (4) the recognition of the evidence of the June 1638 surface faulting plus four previous paleoearthquakes, and (5) the evaluation of its slip rates and return interval. Finally, the relationship of LF with the neighboring faults casts light to the seismotectonic of the region, providing a new insight to the seismic hazard analysis.

**INDEX TERMS:** 7221 Seismology: Paleoseismology; 7230 Seismology: Seismicity and seismotectonics; 7223 Seismology: Seismic hazard assessment and prediction; 8107 Tectonophysics: Continental neotectonics; 8010 Structural Geology: Fractures and faults; **KEYWORDS:** active tectonics, historical seismicity, paleoseismology, seismic hazard, Italy

**Citation:** Galli, P., and V. Bosi, Catastrophic 1638 earthquakes in Calabria (southern Italy): New insights from paleoseismological investigation, *J. Geophys. Res.*, 108(B1), 2004, doi:10.1029/2001JB001713, 2003.

### 1. Introduction

[2] A crossroad of both people and earthquakes, the Calabrian region is rich with stories of cultures accommodating themselves to a violent seismic landscape. Half of the 10  $M \geq 6.9$  earthquakes that occurred in Italy during the past centuries had their epicenters in the long and narrow Calabrian peninsula (Figure 1). Their scenario of death and destruction often extended from coast to coast, as the abandonment of dozen of villages and the exodus of the survivors toward safer lands recurred each time.

[3] While some of these earthquakes have been related to known or studied active structures of the area, mostly by means of their reciprocal geometric relationships (i.e., epicentral area versus fault location) [Monaco and Tortorici,

2000], but also of paleoseismological analyses [Galli and Bosi, 2002], other strong earthquakes are still lacking the identification of their causative fault. In northern Calabria, as exception to this rule, the Castrovillari fault (1 in Figure 1) [Bousquet, 1973] surely ruptured during the historical period [Cinti *et al.*, 1997], although its effects were not recorded by any primary source.

[4] As for the sector resting between the Catanzaro and the Sibari straits (Figure 1), a strong seismic sequence occurred between March and June 1638, with 2 main shocks on 27 March and 9 June (see top of Table 1). The catastrophic 27 March event struck a thickly populated area between the high Crati Valley and the Catanzaro strait area, while the second one devastated the Ionian hillslope of the Sila massif. Until now, no conclusive data have been provided to relate these  $M \cong 7$  earthquakes to possibly active structures, even though Moretti [2000] links the March shock to the Lamezia-Catanzaro fault (6 in Figure 1).

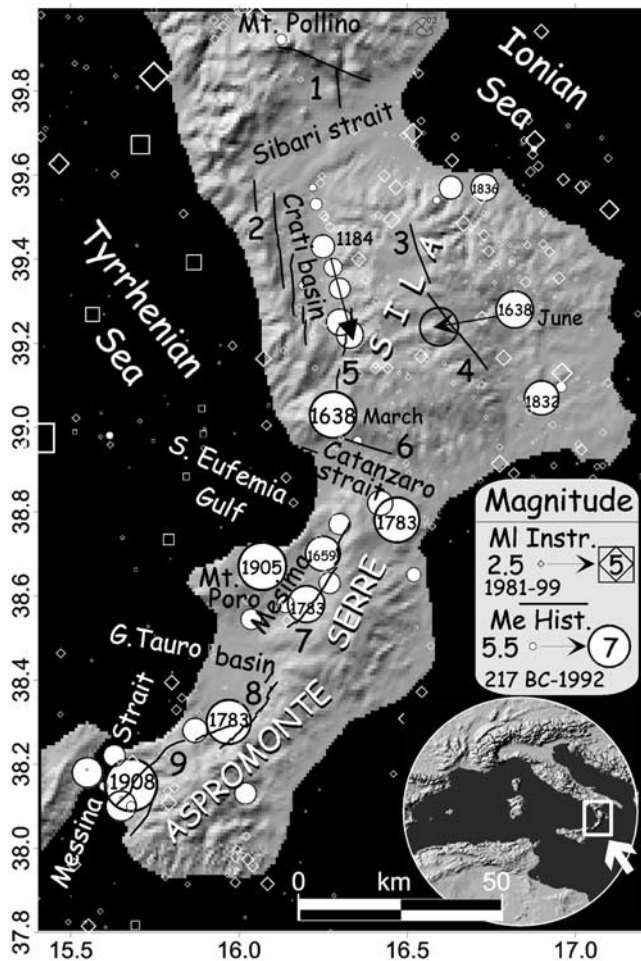


**Figure 1.** Shaded relief of Calabria showing both historical and instrumental seismicity (respectively from Working Group CPTI [1999] and courtesy of I. Guerra, University of Calabria). The latter is mainly confined in the upper crust (rhombs, depth <20 km), with few events localized at greater depth (depth >40–50 km, square symbols). The empty circle in Sila is our proposed epicenter for the 9 June 1638 event. Bold lines are known active faults: 1, Castrovillari; 2, Crati; 3, Cecita Lake; 4, Lakes; 5, Piano Lago–Savuto; 6, Lamezia-Catanzaro (Santa Eufemia–Feroletto); 7, Serre; 8, Cittanova; 9, Delianova-Armo, Reggio Calabria. Modified from Galli and Bosi (2001).

[5] In this paper we focus mainly on the June shock area, both reanalyzing all the available historical sources and by means of geological and geomorphological field survey. Inside a wide area indicated by the contemporary sources, we individuated a previously unknown fault, whose footwall dams small and large streams, creating lakes and ponds (Lakes fault (LF)). We opened four trenches across this fault, which show evidence for repeated displacement events dated back to the 1638 and to previous unknown earthquakes.

**2. Geological and Seismotectonic Framework of Calabria**

[6] Calabria is the southern termination of the Apennine peninsular chain, resting in the toe of the Italian “boot.”

The Apennines formed above a west-dipping subduction zone and consist of a thrust belt–foredeep system which migrated eastward as a response to the flexure-hinge retreat of the subducting foreland lithosphere. This retreat was characterized by slip vectors largely exceeding the average plate convergence rate in the Central Mediterranean region during Neogene and Quaternary times [Patacca and Scandone, 2001, and references therein]. Specifically, the Calabrian arc lies above a NW-dipping subduction slab (i.e., Ionian oceanic lithosphere), well characterized by a Benioff plane [Amato et al., 1993], and extending at least 500 km into the asthenosphere below the southern Tyrrhenian Basin. The latter is commonly considered the back arc basin of the Apenninic subduction, its ages being younger when moving eastward [Gueguen et al., 1997, and references therein]. The Neogene–Quaternary evolution of the Calabrian arc induced a zone of crustal disequilibrium at the boundary between the uplifting Aspromonte–Sila mountain chain (25–45 km thick continental crust) [Ghisetti and Vezzani, 1982] and the subsiding Tyrrhenian basin (10 km thick crust of suboceanic composition) (Figure 2) [Finetti and Morelli, 1973], causing extensional faulting in the imbricate systems of the thrust belt since lower Pliocene time. As a result, a series of elongate N-S and NE-SW trending basins formed on the inner margin of the belt (Crati Valley, Mesima Valley, Gioia Tauro, Santa Eufemia, and Messina Strait basins) (Figure 1), bordered, respectively, by primary east and NW-dipping high-angle normal faults along the Tyrrhenian west coast of southern Italy [Tortorici et al., 1995; Galli and Bosi, 2002]. On the other hand, active thrusting is restricted in a narrow band along the eastern Apenninic front (inset A in Figure 2) as suggested by geophysical profiles [Finetti and Morelli, 1973; Barchi et al., 1998] and instrumental seismicity.

[7] Starting from middle Pleistocene, Calabria was rapidly uplifted, as suggested by the deposition of thick sandy and conglomeratic bodies of deltaic or littoral environment directly overlaying marine clays [Moretti and Guerra, 1997]. These deposits are found at elevation of 400 m asl within the extensional basins (i.e., Crati half-graben basin), whereas Pliocene–Pleistocene sediments and contemporary continental paleosurfaces may reach 1400 m asl in the raised blocks of Sila, Serre, and Aspromonte. According to some authors [Westaway, 1993; van Dijk and Scheepers, 1995], the rapid uplift and the extensional

**Table 1.** Parameters of the Main Shocks of March and June Seismic Sequence According to Working Group CPTI [1999]<sup>a</sup>

Date	Area	Coord.	Io	Imax	Me
<i>Working Group CPTI [1999]</i>					
March 27	Calabria	39.03, 16.28	11	11	6.98
June 8	Crotonese	39.28, 16.82	9.5	10	6.78
<i>This paper</i>					
March 27	Savuto basin	39.11, 16.27	11	11	6.8
March 28	Western Serre range	38.68, 16.23	9.5	10	6.6
March 28	Santa Eufemia plain	38.96, 16.26	11	11	6.6
June 9	Eastern Sila	39.22, 16.57	(11)	9.5	6.7

<sup>a</sup>The bottom of the table anticipates the results gathered in this paper. Me is the Macroseismic Equivalent Magnitude, estimated by using the program “Boxer” [Gasperini, 1999]. Due to cumulative damage effects, we consider the Me of the March events a maximum value.

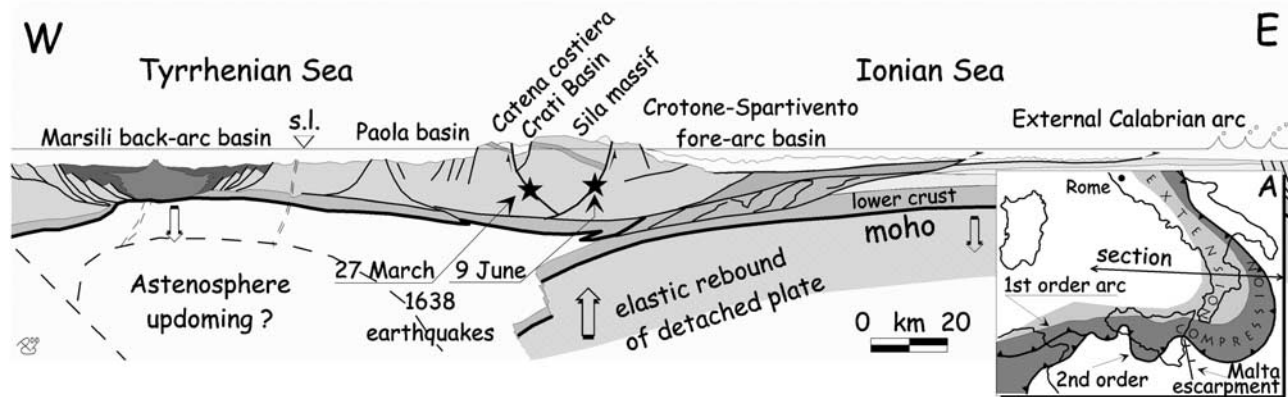


**Figure 2.** Interpretative W-E geological cross section through northern Calabria, from the Tyrrhenian Sea to the Ionian Sea. Black stars indicate the possible hypocenters of the two 1638 main shocks, occurred within the extending upper crust of the Calabrian arc (see inset A for location [modified after Van Dijk and Scheepers, 1995]).

faulting in the Calabrian Arc during late Pleistocene to Recent are a result of the isostatic rebound that occurred when the detached remnants of the ruptured slab started to sink, whereas the nondetached portion rapidly unbent, and elastically bounced upwards (e.g., Figure 2). For this debated issue, see also criticism in the study of *Giunchi et al.* [1996].

### 2.1. Overview of Seismicity and Seismogenetic Faults of Northern Calabria

[8] Calabria is one of the most seismic areas of the Mediterranean region, and has been struck in the past by the most catastrophic earthquakes ever occurred in Italy. In fact, at least 19 earthquakes with  $M \geq 6$  occurred since 91 B.C. between the Messina Strait and the Crati Valley, the last ones being the disruptive 1905 ( $M_s = 7.5$ ) Mt. Poro and 1908 ( $M_s = 7.3$ ) Messina earthquakes (parameters derived from *Working Group CPTI* [1999, Figure 1]). Although the Italian seismic catalogue spans over the past 2 ka (being roughly complete, for destructive earthquakes, in the past 7–10 centuries) [*Stucchi and Albini*, 2000], almost all the Calabrian recorded events are concentrated in less than 3 centuries between 1638 and 1908, and they often occurred within a few months or years of one another (e.g., March and June 1638, February–March 1783, and 1905–1908) or within 1 century (southward migrating sequence of Crati Valley of 1767, 1835, 1854, and 1870) (see triangle-head arrow in Figure 1). Differently from southern Calabria, where all major earthquakes have been related to primary NE-SW normal faults (7–9 in Figure 1) [see *Tortorici et al.*, 1995; *Jacques et al.*, 2001; *Galli and Bosi*, 2002], the northern Calabria seismogenetic framework is still poorly constrained and debated.

#### 2.1.1. Western Sector

[9] As shown in Figure 1, the sector resting between the Catanzaro and the Sibari straits is affected by a  $M \leq 6$  seismicity, which is commonly linked to the Crati basin normal faults (2 in Figure 1). See also focal mechanisms 1 and 6 in Figure 3. For the Crati faults (total length about 40 km) (1–3 in Figure 3) [*Tortorici et al.*, 1995], which drove the opening of the Crati “half-graben” basin during lower middle Pleistocene, no displacements of any upper Pleisto-

cene–Holocene deposits are known. High rates of Upper Pleistocene vertical slip (0.6–0.9 mm/yr) [*Tortorici et al.*, 1995] are mainly inferred from geomorphic features, consisting of deeply eroded relict fault facets, that were likely formed during an earlier time of higher rates of activity. On the other hand, the lack of conclusive evidence of active tectonic along these faults could be explained by their moderate historical seismicity ( $M \leq 6$ ), although we might have lost a strong event in the “short” historical record.

[10] Major problems arise in the southern prosecution of the Crati plain (high Crati-high Savuto basins), where  $M > 6$  earthquakes did occur (27 March 1638 and 10 April 1870), but no active structures have been yet clearly identified (Piano Lago and Savuto–Decollatura normal faults?) (7 in Figure 3) [*Moretti*, 2000].

#### 2.1.2. Central and Eastern Sector

[11] As for the eastern side of the region, few strong events occurred along the Ionian slopes of Sila. Apart from the 9 June 1638 (the epicenter of which has been shifted westward in this paper), they are the 1832 ( $M_e = 6.5$ ) and 1836 ( $M_e = 6.2$ ) earthquakes ( $M_e$  is the Macroseismic Equivalent Magnitude evaluated by *Working Group CPTI* [1999] by using the “Boxer” program in the study of *Gasperini* [1999]). At present, no hypotheses concerning their causative faults exist, although the Highest Intensity Datapoints Distribution (HIDD) and some historical accounts could suggest a relationship between the 1836 event and an E-W lineament (dashed line 4 in Figure 3) (see also Corigliano-Rossano lineament in the study of *Moretti* [2000]).

[12] The Sila massif is instead a historically silent, closed window on the seismotectonics of the region. Only recently the distribution of the instrumental seismicity (Figure 1, courtesy of Prof. I. Guerra, University of Calabria) showed scattered  $M < 4.5$  events even inside the massif itself. Nevertheless, the lack of historical seismicity in the Sila massif should not imply the nonexistence of active structures. An example is given by the NNW-striking Cecita Lake fault (CLF) (5 in Figure 3), newly “appeared” in the literature [*Sorriso-Valvo and Tansi*, 1997], and defined active during the Pleistocene by *Moretti* [2000], or by the “unknown” LF (6 in Figure 3), which is responsible for

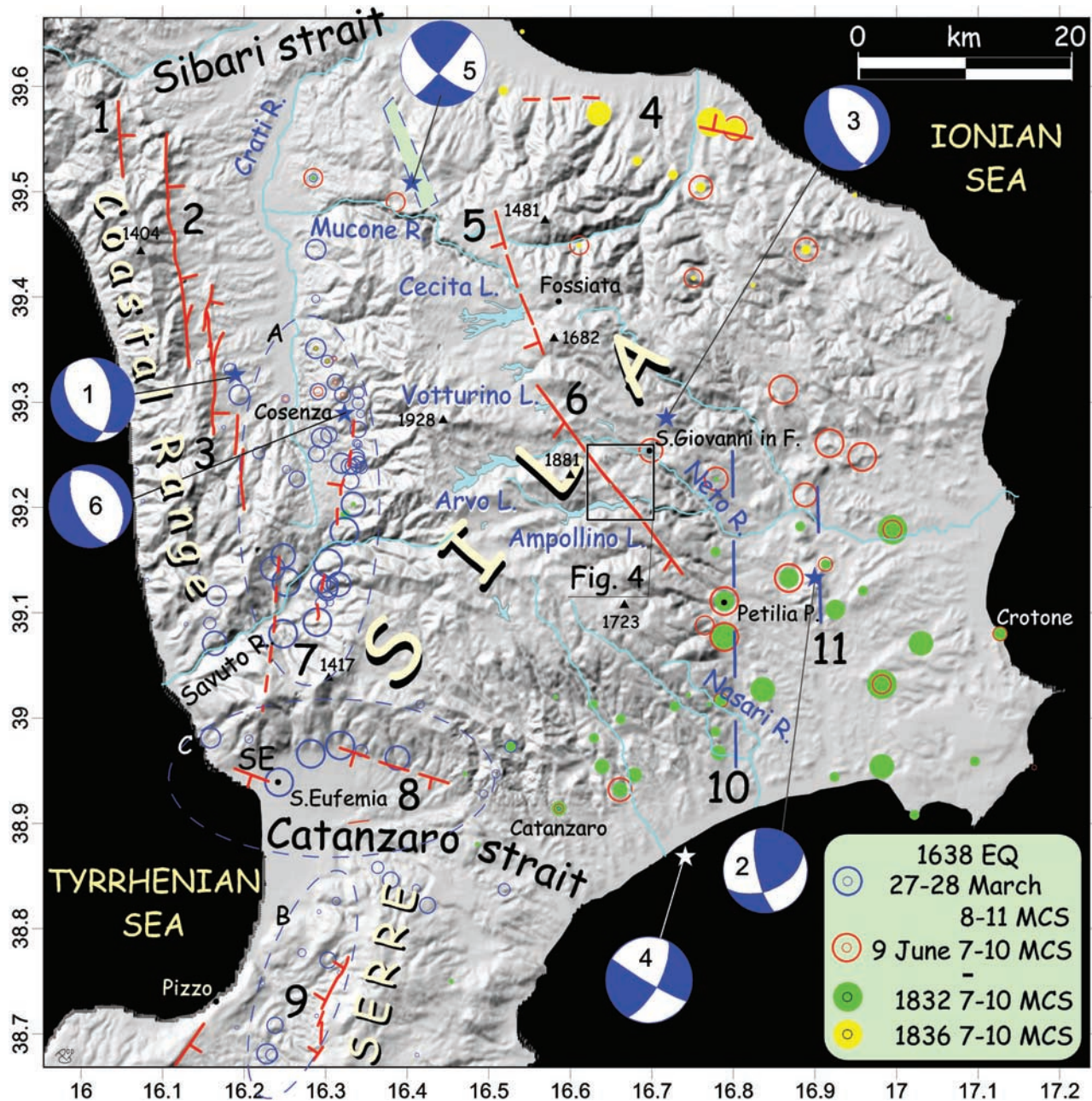


**Figure 3.** Shaded relief of northern Calabria. Our HIDD of 1638 events is shown together with that of 1832 and 1836 (modified from *Boschi et al.* [2000] and *Monachesi and Stucchi* [1998], respectively) (intensities proportional to dimension of circles; see symbols in legend). Note the vast HIDD scattering of the June 1638 event compared to the March one. Dashed ellipses A–C show tentatively the epicentral areas of the three main shocks occurred between 27 and 28 March 1638. Blue stars are the location of the main instrumental events ( $ML = 4-4.5$ ) recorded by the local seismic network of Cosenza University (courtesy of I. Guerra) with related focal mechanisms (1, 20 February 1980,  $ML = 4.3$ ; 2, 24 January 1990,  $ML = 4.5$ ; 3, 24 April 1991,  $ML = 3.9$ ; 4, 26 March 1994,  $ML = 4.1$ ; 5, 27 April 1996,  $ML = 4.0$ ; 6, 18 October 2001,  $MW = 4.4$ ). For the northernmost event (27 April 1996,  $ML = 4$ ), we show also the swarm distribution (green area), which fits with the NNW-SSE plane solution. Red lines are the primary, possibly active faults of the region (teeth on downthrown block), as deduced from literature [e.g., *Tortorici et al.*, 1995] and from our data. 1, Fagnano-Castello; 2, San Marco-San Fili; 3, Montaldo-Rende; 4, Rossano-Calopezzati; 5, Cecita Lake; 6, Lakes; 7, Piano Lago–Decollatura; 8, Feroletto–Santa Eufemia; 9, W-Serre. Blue lines 10 and 11 represent the Marchesato and Mt. Fuscaldo faults according to *Moretti* [2000].

the June 1638 earthquake, as described in detail in the following chapters.

[13] On the other hand, according to *Moretti* [2000], the primary faults of the Ionian slope of Sila are the Marchesato and Mount Fuscaldo faults (10 and 11 in Figure 3), which drove the lowering of Ionian block and which would have been also the causative structures of the June 1638 event. However, apart from the 100 m offset of Lower Pleistocene deposits along the Mt. Fuscaldo fault [*Moretti*, 1993], no displacements of any upper Pleistocene–Holocene deposits are known.

### 2.1.3. Southern Sector

[14] The southern edge of both Sila massif and of Coastal Range is the Feroletto–Santa Eufemia fault (8 in Figure 3), highlighted by a prominent south-facing fault scarp, composed by several discontinuous E-W and ESE-WNW strands with a sinistral en echelon arrangement. According to *Moretti* [2000], the fault is related to a deep transform structure (Catanzaro fault) [*Finetti and Del Ben*, 1986], and it offsets Upper Pleistocene–Holocene terraces, being responsible for the northernmost main shock of the 1783 catastrophic sequence (28 March,  $M_e = 7$ ).

## 3. The 1638 Earthquake Sequence

[15] As mentioned before, the 1638 earthquakes hit the Upper Crati–Savuto valleys, the Catanzaro Strait and the Upper Mesima Valley in March, whereas in June struck the Ionian side of Sila Massif (Figures 1, 2, and 3). Although our geological investigation concerns mainly the June shocks area, we reexamined the whole historical accounts of the seismic sequence, the complexity of which has been interpreted as due to rupture of different faults.

### 3.1. The March 1638 Earthquake

[16] The earthquake of 27 March 1638 ( $I_o = 11$  MCS, Mercalli Cancani Sieberg scale, and  $M_e = 7$ ) is surely the most catastrophic event which hit this portion of Calabria during the historical period (Figure 3), its disruption echoes reaching the farthest country of Europe [e.g., *Parker*, 1638; *Descriptive relation*, 1638; *Dreadfull newes*, 1638]. In the whole the earthquake destroyed more than 100 among villages and hamlets, causing between 10,000 and 30,000 casualties, while several surface breaks, landslides, liquefactions and sinking have been reported by many primary sources to have occurred in different places.

[17] Actually, the analysis of all the most significant contemporary sources [e.g., *Bianchi*, 1638; *Capecelatro*, 1640a, 1640b, 1640c; *D'Amato*, 1670; *D'Orsi*, 1640; *Kircher*, 1665; *Recupito*, 1638; *Vera relatione*, 1638; *Compassionevole relazione*, 1638] allowed us to define at least three separated epicentral areas (Table 1). The northern and most severe one ( $I_o = 11$  MCS) (ellipse A in Figure 3) is located between the upper Crati and the Savuto valleys; the second one ( $I_o = 9.5$  MCS) (ellipse C in Figure 3), less defined although greatly elongated, between the southern part of the Catanzaro strait and the western slope of the Serre range; the third one ( $I_o = 11$  MCS) (ellipse B in Figure 3) could be drawn along the northwestern sector of the Catanzaro strait. According to the account of the Jesuit Athanasius Kircher [*Kircher*, 1665], who was travelling

over the zone struck by the earthquakes, while the first and main shock occurred effectively at the sunset of 27 March, the second and third area were hit only on the Palm Sunday (28 March), when he personally witnessed the disruption and the sinking of Santa Eufemia (see location in Figure 3): “The day after [the earthquakes of 27], Palm Sunday, [between Pizzo and Santa Eufemia]...we heard a rumbling sound like a thunder, quite hollow, which seemed coming from a far place, but that was growing louder as approaching nearer, until it stopped in the underground of the place on which we stood. And just there it struck the Earth with a so violent shake that everyone, being unable to stand, was compelled to catch hold of a branch, or a sea shrub...And there, exactly in that moment, occurred the ruin of the celebrated town of Santa Eufemia...As the Nature's fury lessened, and we cast a glance around, we saw the aforementioned town surrounded by a great cloud...But, at three of the afternoon, after the cloud lazily passed away, we turned to look for the city, but did not see it: nothing, but a dismal and putrid lake was seen where it stood. We looked about to find some one that could tell us of this sad catastrophe, but could see no person...Only an astonished child, sitting on the shore...refusing the food that we offered him...seemed to point out with his fingers the catastrophe of Santa Eufemia” [*Kircher*, 1665, translated from Latin by the authors].

[18] Consequently, the magnitude of each shock is obviously smaller than the one provided by *Working Group CPTI* [1999] (the parametric earthquake catalogue of Italy). In particular, on the basis of the HIDD of the upper Crati–Savuto area event (27 March) we estimated  $M_e = 6.6$  (by using the “Boxer” program) [*Gasperini*, 1999]. Nevertheless, this magnitude should be considered a maximum value, since the used HIDD contains also the cumulated effects of the two 28 March events.

[19] Summarizing, on the basis of the HIDD we can hypothesize that three different fault systems ruptured from north to south between 27 and 28 March: these could be hypothetically related to the Piano Lago and Savuto–Decollatura faults (7 in Figure 3) [e.g., *Moretti*, 2000], the Santa Eufemia–Feroletto fault (8 in Figure 3, which is part of the Lamezia–Catanzaro fault in the study of *Moretti* [2000]) and the northern prosecution of the Mesima fault (9 in Figure 3) [see *Monaco and Tortorici*, 2000; *Galli and Bosi*, 2002]. Nevertheless, no conclusive field data have been yet collected concerning the causative faults of the March events.

### 3.2. The June 1638 Earthquake

[20] “During the night [of 9 June 1638; this event is reported on 8 June on *Working Group CPTI*, 1999; see also *Chiodo et al.*, 1995] a horrible earthquake struck towns, lands and castles, lowering mountains, rupturing the Earth surface and opening long fractures.” This is the rough translation from Lutio D'Orsi [*D'Orsi*, 1640], who described the effects of the June event, the catastrophic earthquake which struck an area located few dozen kilometers away from the epicentral region of 27 March, on the opposite, eastern slope of Sila. This event has been recently studied by *Chiodo* [1993] and *Scaccianoce* [1993].

[21] The 9 June earthquake was preceded at dawn and noon of the day before by two strong foreshocks that

alerted the population, convincing those few still sleeping in their home (since March the Earth was trembling continuously) to get a safe shelter far away from the villages, in the country. Therefore, in spite of the damage level, the official death toll is cited as just over a few dozens.

[22] On the basis of all the known primary historical sources, we reevaluated the MCS intensity for each village (Table 2 and Figure 3), estimating an  $I_{max} = 9.5$  (MCS) (Table 1). Six villages were almost completely destroyed, whereas about twenty scattered in a vast area elongated about 60 km from south to north had  $I \geq 8$  MCS. The HIDD surrounds at north, east, and south the Sila massif, reflecting the absence of villages in the mountainous area, a wild and inhospitable plateau with elevations ranging between 1300 and 1900 m asl. It is worth to note that while part of the damage could be interpreted as cumulative on that caused by the March event, part could be underestimated (e.g., south and western sector) due to the previous level of disruption of buildings which did not allowed to “record” further damages (“if it did not cause a new slaughter it was because it found few places to beat down on”) [Bernardo, 1639]. In any case, due to the location of the epicenter in a mountainous and uninhabited area, the  $I_0$  value should be reasonably higher than the evaluated  $I_{max}$ .

[23] In contrast to the 27 March event and to several studied case histories [e.g., Galli and Galadini, 1999], the June HIDD does not depict any particular trend which could highlight the causative fault. It is our feeling that many factors contributed to the complexity and difficult understanding of the 9 June HIDD: (1) site effects (due to the extremely varied geology and to the scarce geotechnical properties of the Tertiary and Quaternary rocks of the eastern coast), (2) gravity-driven phenomena (triggered by shaking, as reported by many historical sources), (3) vast uninhabited areas, and (4) cumulative damage with the two strong foreshocks of 8 June (and with the 27 and 28 March events).

[24] Anyway, the most important issue highlighted by the contemporary sources is the opening of an impressive fracture across the Sila massif, the description of which we translated from Latin and the old Italian as:

1. “... in the mountain named Sila in that day a very long and deep fracture opened due to the earthquake...” [Relazione del terremoto, 1638].

2. “... in the land of San Giovanni in Fiore the ground ruptured for a width of 2 palms [about 50 cm], for the length of many miles toward the Sila...” [D’Orsi, 1640].

3. “... from the border of Policastro to the extreme side of the mountain [Sila], northward, the ground lowered 3 palms [about 80 cm] by one side, along a 60 miles long straight line, and what is wonderful, it did ruptured with the same entity both in the lowermost valley and in the highest mountain...” [Di Somma, 1641].

4. “... the earthquake...opened chasms...in the most uninhabited mountains of the Sila, which sent out flames...” [Paragallo, 1689].

5. “... the ground was offset by 3 palms along a 60 miles long space from the Policastro border to the Sila of Cosenza [see Di Somma, 1641], and it happened to me to see it again, after many years, in the Sila in a place named Cagno...” [Martire, 1704].

**Table 2.** Highest Intensity Datapoints ( $I \geq 7-8$ ) of the 8 June 1638 Event Evaluated on the Basis of All the Primary Historical Sources<sup>a</sup>

Locality	I (MCS)
Casabona	9.5
Mesoraca	9.5
Policastro	9.5
Verzino	9.5
Zinga	9.5
Belvedere di Spinello	9.0
Calciviti (Caloveto)	9.0
Calopezziati	9.0
Crosia	9.0
San Giovanni in Fiore	9.0
Scala Coeli	9.0
Simeri	9.0
Acri	8.5
Bisignano	8.5
Bocchigliero	8.5
Longobucco	8.5
Rocca di Neto Vecchia	8.5
Sant’Angelo di Frigillo	8.5
Cutro	8.5
Belcastro	8.0
Cotrone	8.0
Santa Severina	8.0
Catanzaro	7.5
Zumpano	7.5

<sup>a</sup>Intensities slightly differs ( $\pm 1^\circ$  MCS) from other compilations [e.g., Scaccianoce 1993; Chiodo, 1993; Monachesi and Stucchi, 1998; Boschi et al., 2000]. Acri was not included in the previous studies.

[25] These descriptions are the oldest detailed, and self-consistent historical descriptions of surface faulting around the globe. Actually, the length of the fracture cited as 60 miles (110 km!) by Di Somma [1641], and just referred by late authors] appears unexpectedly long for a  $M_e = 6.7$  earthquake; it could be exaggerated or, more probably, bad typeset from Di Somma’s original manuscript (e.g., in 1600s Italian manuscripts we ascertained that the cursive “2” and “6” are quite similar).

[26] Even if the true length may remain questionable, the overall information reported by all the eye witnesses about location, offset and continuity, both in the valleys and across the ridges, is a robust indication of the tectonic origin of the fracture. Moreover, the persistence of the step after 60 years [Martire, 1704] corroborate this impression.

[27] Another convincing fact is that during our field survey along a lineament (LF) seen on the 1954 air-photo coverage, we found that the local place-name of one area where we were selecting potential trenching site was “Cagno,” the same cited and visited by Martire [1704] (see Figure 4 for location). Moreover, the intriguing circumstance was that the natives, although they have no memory of any earthquakes in the area, still today call this area “a colla u terremotu” (the sag of the earthquake, in the local Calabrian dialect). Similarly, few kilometers away along the same lineament, it exists an area called “Trepidò di luce,” which literally means “it trembled with light” (old Italian *trepidare* = to tremble) (Figure 4).

[28] In the whole, while the vastly scattered HIDD of this event, with several irregularities (i.e., high and low MCS intensities mixed in the same areas) does not show any particular trend that can reflect the bearing of the seismogenic structure, the existence of the long coseismic

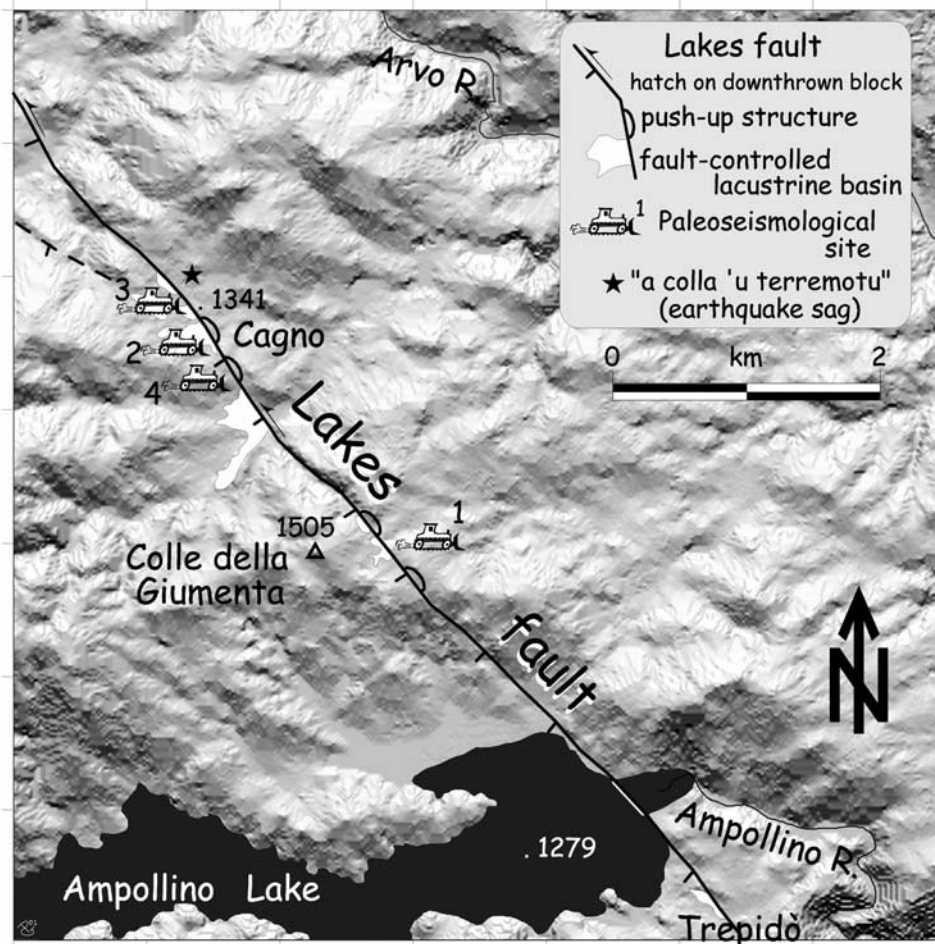


**Figure 4.** Shaded relief of the northern Ampollino Lake area (from original 1:25,000 topographic data, courtesy of Istituto Geografico Militare, aut. 5410 of 6 June 2001). The central strand of LF is drawn together with the four trenching sites. The present lake hides the ancient lacustrine deposits observed by the Royal Geological Survey of Italy in the 19th century [*Regio Ufficio Geologico d'Italia*, 1895].

fracture crossing the inner Sila massif (which we identified with the lineament/fault discussed in the following) (see Figures 3 and 4) casts light both on the littered HIDD and on the causative fault of the June 1638 earthquake.

#### 4. Geomorphology of the Investigated Area

[29] The area is characterized mainly by crystalline units (quartz-diorites, monzonites and granodiorites, together with gneisses and metamorphic limestones) which overthrust the Apennine sedimentary nappes since Miocene. The crystalline rocks are affected by deep and variable weathering profiles, which probably developed during Pliocene and lower Pleistocene, when a vast paleosurface was carved all over the emerged Sila massif [*Dramis et al.*, 1990]. The erosional processes of late Pleistocene–Present (emphasized by the rapid tectonic uplift of Calabria), although prevailing on the weathering ones, were not enough to completely remove the exposed weathered mantle [*Matano and Di Nocera*, 1999]. The present morphology is then dominated by flutes of these remnant surfaces, mantled by thick saprolite and smoothly carved by a complex paleodrainage, which is truncated, reen-

trenched and captured by the present upstream-downcutting network.

[30] The area is also characterized by the presence of several barrier lakes (built since the first half of the 20th century) that occupies ancient lacustrine basins (e.g., Cecita Lake, Arvo Lake, and Ampollino Lake) and by sparse intermountain plains mantled by recent alluvial, colluvial and lacustrine deposits.

##### 4.1. Geomorphological Investigation Along the LF

[31] We restricted our research in the area where the historical descriptions concerning the June event reported the most severe effects and the existence of surficial breaks, that is the eastern Sila massif region, between the rivers Nasari and Neto (Figure 3) [see *D'Orsi*, 1640]. Sila (from Latin *silva* = forest) since the Greek and Roman times has been one of the most thickly forested region of Europe. Thus, rock outcrops are very rare, making geomorphic analyses difficult.

[32] We focused our attention on the lineament seen on air-photos and passing through the Cagno area, a prominent N40°W trending feature, which is transverse to the drainage pattern, and runs both “in the lowermost valley and in the

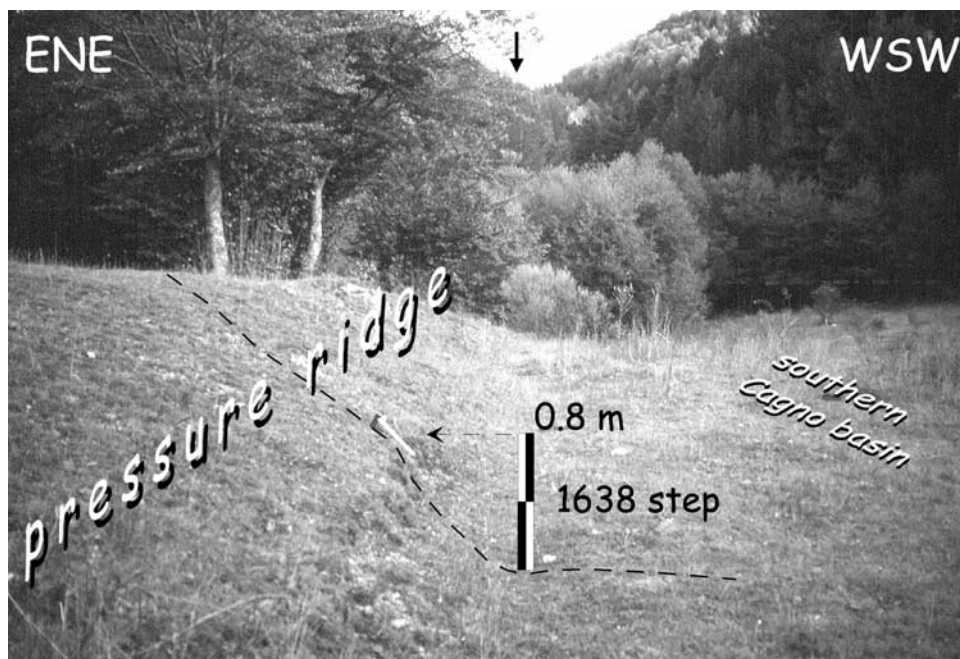


**Figure 5.** View looking south along LF scarp in the Cagno basin. Note the steep scarplet at the base of the pressure ridge, which we relate to the 1638 June event. The arrow in the background indicates the fault trace, which is evidenced by a 2–10 m high scarp (Colle della Giumenta area) (see Figure 4 for location).

highest mountain,” between the borders of the municipality of Petilia Policastro and San Giovanni in Fiore [see *Di Somma*, 1641]. Its surficial expression is visible along about 25 km, being mainly evidenced by a west-facing scarp and/or small ridges, which border (and dam) the eastern edge of several intermountain basins scattered along its hangingwall (Figures 3 and 4). In the southern sector the scarp crosses the head of the Ampollino Lake (formed in 1923 with a capacity of  $67 \times 10^6 \text{ m}^3$ ), few meters upstream of the masonry dam, whereas in the northern part it crosses the eastern edge of another small artificial lake (Votturino Lake,  $3 \times 10^6 \text{ m}^3$ , gravity concrete dam), created on a swampy area. The artificial Ampollino Lake fills the basin of the paleo-Ampollino lake, and entirely hides the ancient lacustrine deposits mapped by the Royal Geological Survey of Italy in the 19th century [*Regio Ufficio Geologico d’Italia*, 1895].

[33] The fault presents smooth bendings with curvature radius  $<1 \text{ km}$ , which are marked by narrow elongate ridges and depressions. These features commonly join up with a horizontal component of the motion (pressure ridge and pull-apart) [e.g., *Galli*, 1999], which we do not exclude to be substantial (Figure 4). On the other hand, there were no clear geomorphic evidence of a long term tectonic control of the landscape, apart from a general deepening of the fluvial network eastward of the fault and the existence of some secondary streams entrenched along the lineament itself.

[34] All over its length, on the field, the fault appears as a scarp carved both in the crystalline rocks and in the alluvial–colluvial deposits, commonly (central sector of LF) (Figure 4) marked by a steep fresh scarplet at the base of the main feature (about 1 m) (Figure 5). The few rocky outcrops in the quartz-diorite units show an intensive tec-

tonic fabric approaching to the scarp, with milonite and argillitic lithons packed between the shear planes.

#### 4.2. Geological Observations Along the CLF

[35] Northwestward to the LF area, another barrier lake exists within the paleo-Cecita lacustrine basin (late lower

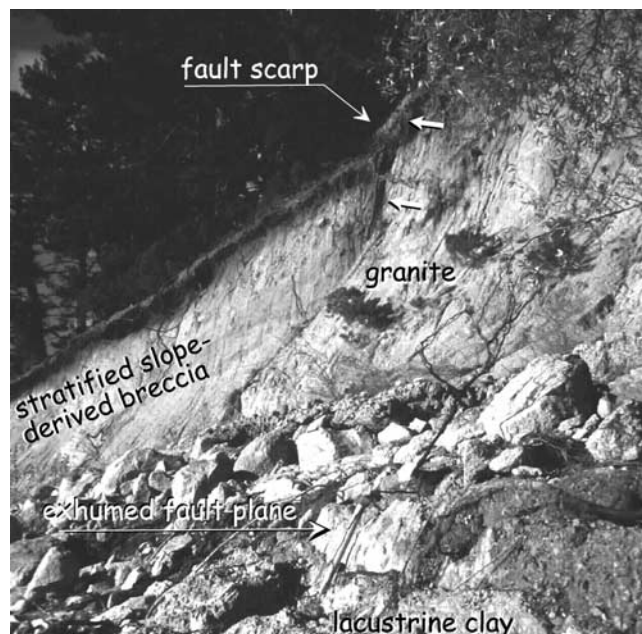


**Figure 6.** View looking north along CLF. In this site, the fault offsets lacustrine clayey deposits (foreground) and slope-derived breccias (background). This outcrop is visible only during the low-standing levels of the lake (i.e., during maintenance works at the dam).

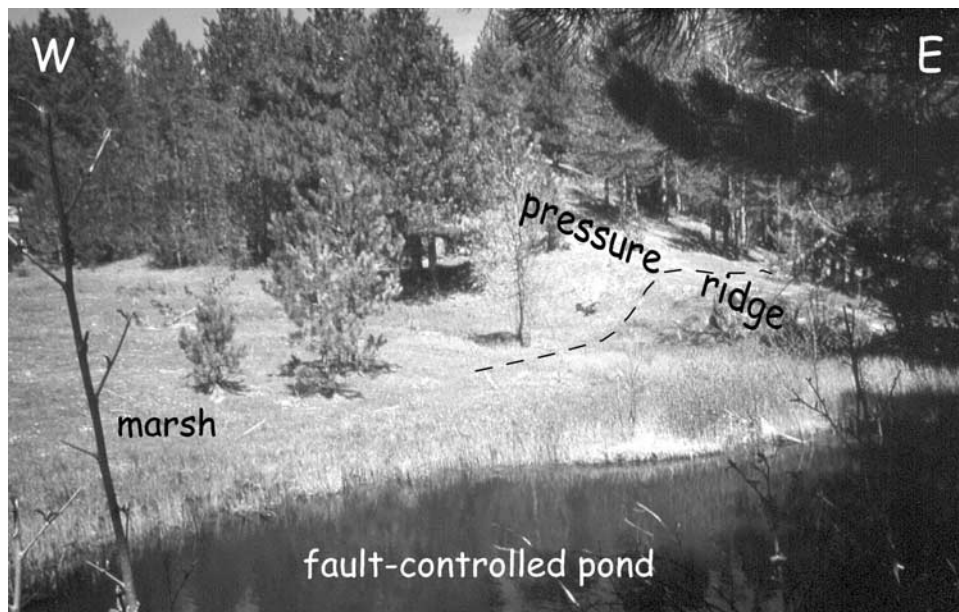


**Figure 7.** View looking north along LF scarp, downhill of Colle della Giumenta. Note the pond formed by the uprising footwall; the water level has been partly lowered by the native-born workers who cut the fault scarp/threshold. The photo was taken from a lacustrine terrace standing 1.5 m above the present water level. We excavated a 4 m deep pit (pit 3) within this terrace, finding a continuous lacustrine-marsh sequence dated back to 4799–4673 B.C. (sample CGLP5). The sequence lays over an important erosion surface carved on older clayey lacustrine beds and characterized by an indurated black soil-crust (age > 41,290 BP, sample CGLP4). We dug trench 1 few meters southward of the pond.

Pleistocene) (Figure 3) [Henderson, 1973; Moretti and Guerra, 1997]. This basin, originally draining toward the Ionian Sea through a saddle located eastward of the Fossiatà area, was captured by the deeply entrenched Mucone River (a tributary of the Crati river) (see Figure 3 for location). Since the entrenching and headward erosion of all the Sila rivers took place after the regional Calabrian uplift (started in the Middle Pleistocene) [Henderson, 1973; Moretti and Guerra, 1997], the paleo-Cecita lake was reasonably drained in the same period.

[36] The present lake (created in the 1950s by means of an arch dam, and with a capacity of  $121 \times 10^9 \text{ m}^3$ ) lies in the hangingwall of a prominent NNW-SSE scarp (facing west), marked by fault planes affecting the basement granites, lacustrine clayey deposits and slope-derived breccias (CLF) (Figure 6). In some places, the fault scarp dams the flow of secondary streams, and creates, analogously to LF, small marsh areas.

[37] The CLF was reasonably responsible for the beheading of the eastern part of the paleo-Cecita basin; the upthrown lacustrine beds outcrop in the Fossiatà area at least 170 m above the relative lacustrine deposits scattered around the present Cecita lake, in the hangingwall [see also Moretti, 2000]. This offset should have taken place after the breakthrough of the Mucone river within the Cecita basin, as evidenced by the comparable thickness of the lacustrine deposits across the fault (i.e., the paleolake was already captured and drained by the Mucone River and no barrage/sedimentation occurred during the progressive uplift of the eastern block of the CLF). According to this hypothesis, which makes no claims to being conclusive, since the entrenching and headward erosion of all the Sila rivers took

place after the regional Calabrian uplift (started in the Middle Pleistocene) [Henderson, 1973; Moretti and Guerra, 1997], the CLF offset could be then occurred during the late Pleistocene (with slip rate in the order of 1 mm/yr).

## 5. Paleoseismic Analyses Along the LF

[38] During April 2001 we decided to open a first 8 m long, 5.5 m deep trench across the strand of the scarp which dams a small lake and a marsh at the foothill of Colle della Giumenta (Figure 4, site 1, and Figure 7). This test site highlighted the presence of faulted colluvial and slope-derived deposits (Figure 8), in tectonic contact with crystalline rocks. Thus, in May we opened 3 other trenches along the fault scarp (trenches 2–4, respectively, 12 m long, 5 m deep; 7 m long, 3 m deep; 4 m long, 2 m deep) in the most geologically favorable area (Cagno basin), plus several other check pits along the fault.

[39] Afterward, 24 samples were sent to Beta Analytic Inc. (Miami, FL) for absolute dating. Table 3 summarizes the accelerator mass spectrometer (AMS) and radiometric (R)  $^{14}\text{C}$  analyses of sampled detrital charcoal and soil/deposit bulk. All the detrital charcoal samples received a standard pretreatment consisting of acid/alkali/acid washes. Samples yielded a wide variety of ages, ranging from  $170 \pm 40$  radiocarbon yr BP to greater to 41,290 yr BP. Conventional ages have been calibrated using program Calib 4.1 [Stuiver et al., 1998]; relative  $1\sigma$  (68%) and  $2\sigma$  (95%) areas under probability distribution are shown on the right side of Table 3, together with the associated value for each age subinterval. In the text and in the trench logs samples have been reported with  $1\sigma$  calendric age; in case of multiple

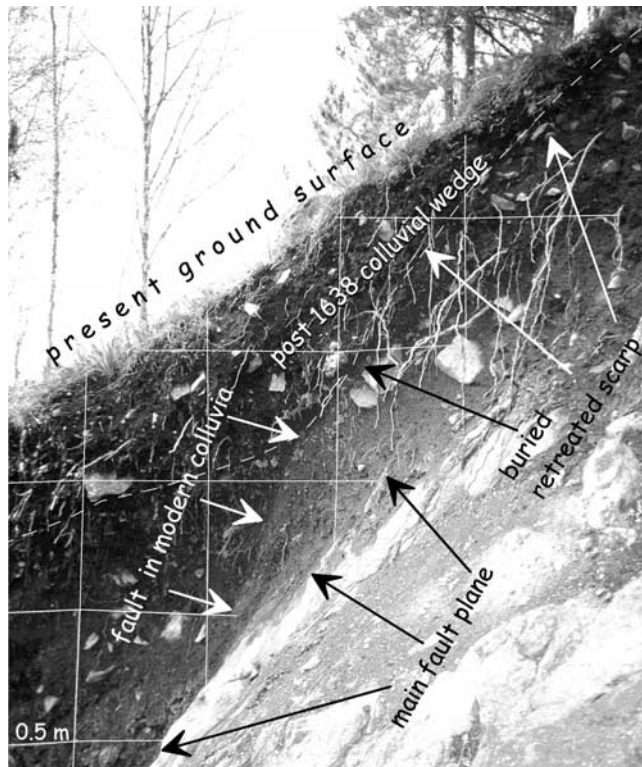


**Figure 8.** Partial view of the northern wall of trench 1 during the excavation phase (see inset in Figure 9). Note the faulting of modern colluvium under the present forest soil. This trench was excavated outside the Cagno basin, along the ridge that runs toward the Ampollino lake (Colle della Giumenta site).

intervals, we adopted the whole  $1\sigma$  range or those intervals characterized by the highest associated probability (minimum 55%, single or grouped).

### 5.1. Trench 1

[40] In this area the fault borders the eastern flank of a narrow and entrenched valley, which crosses uninterruptedly the entire mountain ridge between the Ampollino Lake and Cagno basin. The fault scarp affects granite rocks and shows at the base a striated free-face, 1 m high (pitch  $35^\circ$ – $40^\circ$ ). Close to the divide (eastward bending of the fault at the foothill of Colle della Giumenta in Figure 4), the progressive uplift of the ridge in the past earthquakes led to the formation, and then blocking, of two gorges at the mouth of small elongate basins, that became a barrage behind which ephemeral lake deposits accumulated. At present, the water level of one lake has been raised with an artificial dam, while the other basin is occupied by a marsh (see Figure 7); trench 1 was excavated in the middle of the two. The main fault plane locally strikes  $N50^\circ W$ , dipping  $65^\circ SW$ . Its footwall (Figure 9) is mainly composed by highly fractured granodiorite rocks (unit 9), mantled by orange coarse sands with sparse clasts (unit 3). In the hangingwall a strongly fractured wedge, belonging to unit 9 (unit 8), outcrops in tectonic contact under alternating yellowish and orange silty sands with granite clasts, stratified (unit 6), and a granite-derived rudite (unit 7) (slope-derived deposits). Units 6 and 7 are folded and stretched

along the fault plane, and are truncated by an important erosional surface (ES1). Unit 5, a green coarse silty sand, lays over ES1, passing upward to a sandy gravel with angular clasts (unit 4) and coarse gravel lenses. Units 4 and 5 are truncated by another erosional surface (ES2). Unit 2 is a brown sandy–silty colluvium, with sparse clasts ( $\phi$  max 10 cm), passing upward to a similar deposit (unit 2a) through an erosional surface (ES3) (marked by a thin stone line) which truncates the faint stratification of unit 2. Finally, unit 1 is a blackish pedogenic colluvium, formed by organic silty sands and sparse centimetric clasts.

[41] The age of the succession is constrained by the  $^{14}C$  dating of four samples (Table 3). Unit 4 contains a piece of charcoal dated 3630–3381 B.C. (sample CGL3), whereas units 6 and 7 should be dated back before the climate phase responsible for the development of ES1. Since Galli and Bosi [2002] recognized in southern Calabria an erosion phase truncating 4305–4060 B.C. calibrated age deposits, the reasonable age of this climate phase should be around 4000 B.C. This age agrees with the Holocene cold event 4 of Bond *et al.* [1997], dated slightly after 4000 B.C. and found also by Keigwin and Boyle [2000] and Siani *et al.* [2001]. Sample CGL5 (Unit 2) taken at 30 cm over ES2, gave a date of 215–107 B.C., which should be considered as a minimum age for its deposition (the sample is a colluvial deposit, and thus its age is partly that of its parent material). The top of unit 2a has been dated at 1564–1628 A.D. (charcoal sample CGL7).

[42] Apart from unit 1, all the units are faulted and some are strongly deformed by the fault motions. The last faulted unit is 2a, which implies that the age of the youngest surface-rupturing event is post 1564–1628 A.D. (i.e., 1638 A.D., event horizon EH1). Unit 1 is interpreted as the colluvial wedge filling the 80 cm step (value obtained by restoring unit 2 to form a regular slope profile, assuming that no step existed before 1638) related to this event.

[43] Considering the nature and shape of units 2–2a, we hypothesize that they might represent the colluvial wedge which filled the step of 2 other events, separated by ES3. Thus, a penultimate event tentatively occurred before 1564–1628 but much after 215–107 B.C. (EH2), while the previous one was just before 215–107 B.C. (EH3). However, indication of EH2 are weak, and unit 2a could also represent a not tectonically induced sedimentary wedge. Another event of unknown age might have occurred after the deposition of unit 4 (3540–3500 B.C.), which is cut by fault B, the latter being “sealed” by ES2 (well before 240–100 B.C.) (EH4). Other Holocene events are then witnessed by the folding which affects the deposits below ES1 (units 6 and 7), surely prior to 3540–3500 B.C. (EH5), and by the intense shearing of unit 8.

### 5.2. Trench 2

[44] This trench was excavated in the Cagno basin where the fault, bending slightly eastward, forms a narrow ridge which dams the eastern side of the basin (site 2 in Figure 4) (Figure 10). The villagers have reinforced and reconstructed the eroded part of the natural dam in order to create a small pond (which we necessary dry up by excavating a 80 m long and 1–3 m deep canal). The ridge (Figure 10) (local strike  $N20^\circ W$ ), is mainly composed by leukogranites and granodiorites, highly fractured and weathered. The crystal-

**Table 3.** Laboratory and Calibrated Radiocarbon Ages of Samples From Trenches 1–4<sup>a</sup>

	Sample	Analysis	Dated Material	<sup>14</sup> C Age (1-σ) (Radiocarbon years BP)	Calendric Age Range (1s-68%)	Area (%)	Calendric Age Range (2s-95%)	Area (%)
Trench 1	CGL3	AMS	charcoal	4730 ± 50	3630–3578 B.C.	38.8	3638–3495 B.C.	63.3
					3538–3503 B.C.	23.8	3467–3374 B.C.	36.7
					3428–3381 B.C.	33.1		
	CGL5	R, BLC	organic silt	2160 ± 70	356–288 B.C.	34.2	383–44 B.C.	100
	CGL7	AMS	charcoal	360 ± 40	215–107 B.C.	52.7		
Trench 2	CAGS1	AMS	charcoal	1180 ± 40	1476–1523 A.D.	44.4	1450–1533 A.D.	46.4
					1564–1628 A.D.	55.6	1539–1636 A.D.	53.6
	CAGS3	AMS	charcoal	1390 ± 50	780–794 A.D.	12.9	771–904 A.D.	78.8
					798–893 A.D.	87.1	911–976 A.D.	18.8
	CAGS3B	AMS	charcoal	490 ± 40	616–682 A.D.	96	559–695 A.D.	92
					1410–1442 A.D.	100	1396–1476 A.D.	96
	CAGS4	AMS	charcoal	1350 ± 40	645–691 A.D.	88	637–726 A.D.	82.8
							738–773 A.D.	14.6
	CAGS4B	AMS	organic silt	2620 ± 50	831–765 B.C.	100	900–758 B.C.	86
					1666–1686 A.D.	15.6	1660–1700 A.D.	17.3
CAGS6	AMS	charcoal	170 ± 40 <sup>1</sup>	1730–1782 A.D.	41.5	1727–1816 A.D.	43.6	
				1786–1809 A.D.	10.3	1915–1955 A.D.	18.1	
CAGS7	AMS	charcoal	1710 ± 50	1925–1949 A.D.	17.7			
				258–283 A.D.	22.8	214–434 A.D.	99	
Trench 3	CAG01	R, EC	charcoal	3440 ± 120	320–398 A.D.	67.7		
					1892–1603 B.C.	97	2036–1490 B.C.	98
	CAG02	AMS	charcoal	2970 ± 40	1261–1186 B.C.	55.3	1316–1047 B.C.	98
					1184–1127 B.C.	42.2		
	CAG03	AMS	charcoal	3200 ± 40	1507–1433 B.C.	100	1528–1395 B.C.	98
					1405–1260 B.C.	97	1440–1187 B.C.	93
	CAG04	AMS	charcoal	3060 ± 60	1430–1365 B.C.	49.5	1515–1255 B.C.	94
					1365–1296 B.C.	47.3		
	CAG17	AMS	charcoal	3190 ± 50	1515–1427 B.C.	99	1533–1374 B.C.	93
					1387–1382 B.C.	49.3	1410–1211 B.C.	97
	CAG19	AMS	charcoal	3050 ± 40	1322–1286 B.C.	31.6		
1284–1261 B.C.					19.1			
Trench 4	CAGC1	AMS	charcoal	2530 ± 40	792–759 B.C.	26.7	800–535 B.C.	97
					683–663 B.C.	13.9		
					640–588 B.C.	36.3		
					581–545 B.C.	26.1		
					1182–1299 A.D.	96	1152–1327 A.D.	81
					776–900 A.D.	78.6	705–754 A.D.	10.7
					918–959 A.D.	21.4	756–985 A.D.	86.7
Pit 3	CGLP2	R, EC	charcoal	590 ± 60	1304–1366 A.D.	75.4	1294–1429 A.D.	100
					1385–1405 A.D.	25.6		
					–	–	–	–
CGLP4	R, EC	organic silt	>41,290	–	–	–	–	
				–	–	–	–	
CGLP5	AMS	charcoal	5860 ± 60	4799–4673 B.C.	90	4812–4550 B.C.	94	

<sup>a</sup>R means Radiometric standard analysis; BLC, Bulk low carbon; EC, extended counting; AMS, Accelerator Mass Spectrometry.

line rocks outcrop both in the footwall (unit 9 in Figure 11) and hangingwall (units 7 and 8) of the fault, even if with a different metamorphic *facies*. Between units 7–9, a strongly deformed and multifaulted wedge of different sedimentary units is packed, the geometry and fabric of which account for a not negligible horizontal component of slip (flower structure feature). Moreover, the fault plane, which dips 50°W, shows few striations with a pitch of 40° (sinistral). On the opposite wall of the trench (south), this tectonic wedge is much thinner and is represented only by squeezed grayish blue lacustrine clays (unit 6). Units 3–5 are colluvial deposits, mainly composed by gravel to coarse sands, which are difficult to correlate one to each other across the several fault planes. Units 2 and 1-1a, far away from the fault zone, are respectively orange silt–sandy colluvia and brownish marsh silt–sandy deposits, both with sparse clasts and charcoals. Unit 1 lays over a blackish indurated silty level rich in clasts, which is a paleosol developed on an erosional surface (ES1) which truncates unit 2. Although units 1-1a are quite similar, they are separated by a thin and discontinuous stone line, unit 1a being less dense and slightly finer. This stone line proceeds toward ENE as an

erosional surface over unit 2 (ES2). We followed unit 1a westward along the long drainage canal, which we excavated to dry up the pond, until it thickens and joins with the present marsh deposit.

[45] The age of the deposits is constrained by seven <sup>14</sup>C dates of as many samples: unit 1a is younger than 1666–1782 A.D. (sample CAGS6) (age falling in a plateau of the calibration curve: 2σ interval reaches 1955 A.D.) [Trumbore, 2000] and it is currently in sedimentation. Unit 1 was deposited after 320–398 A.D. (sample CAGS7) and during 612–686 and 1410–1442 A.D. (samples CAGS3 and CAGS3b). Unit 3, which fills two open fractures along faults B and C, yielded a date of 798–893 A.D. (sample CAGS1) and 645–691 A.D. (sample CAGS4), while unit 6 yielded a date of 831–765 B.C. (CAGS4b, age of the bulk of the lacustrine clays).

[46] All the deposits close to the fault plane are faulted, and then the last event is after 798–893 A.D. (sample CAGS1) (EH1). Moreover, the coseismic footwall uplift and the consequent barrage of the basin outlet (see Figures 4 and 9) likely caused the raising of the water table and the growth of a marsh environment in the hangingwall (cur-

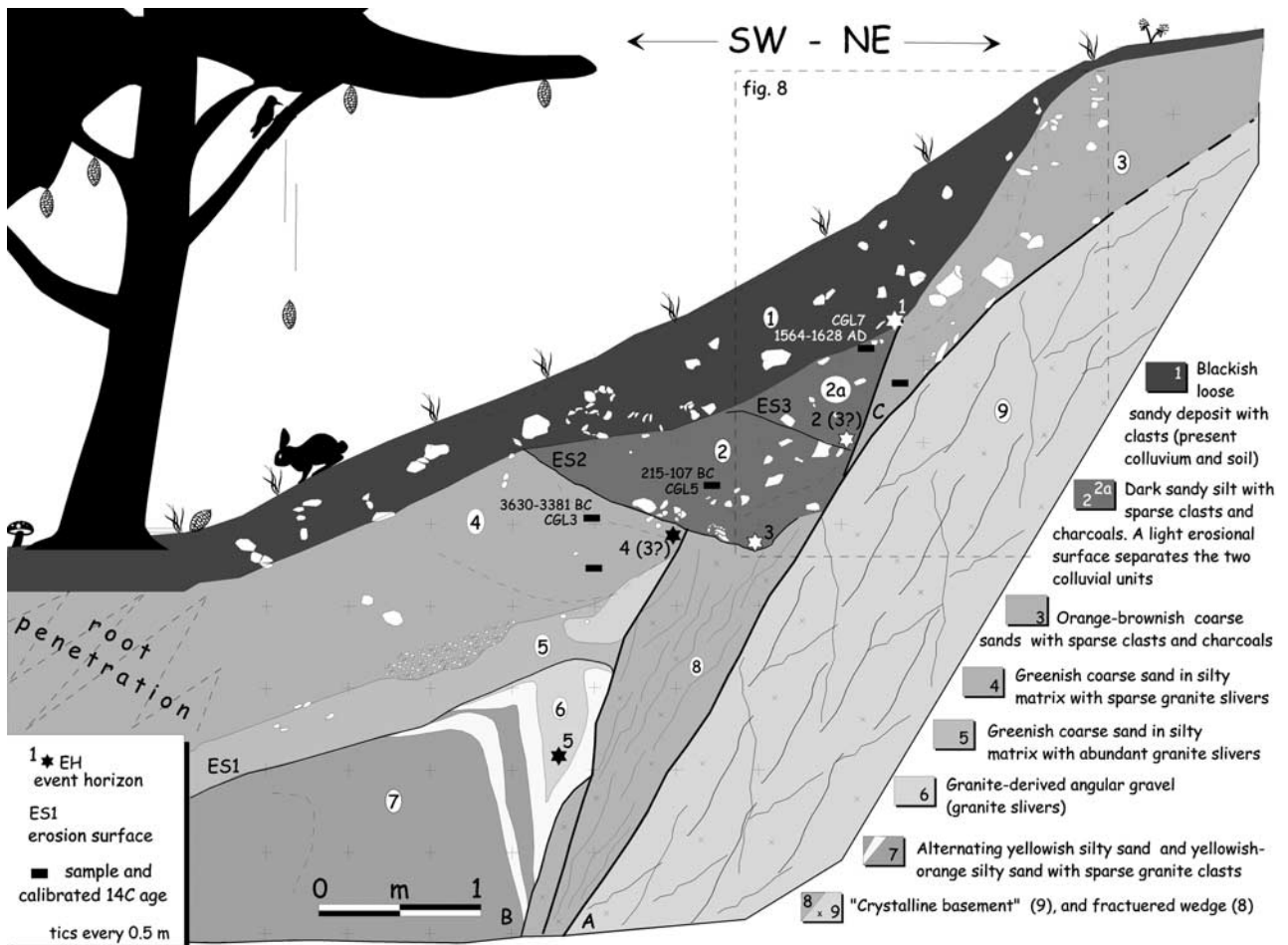


**Figure 9.** Sketch of northern wall of trench 1. Fault C (see inset of Figure 8) cuts a modern colluvium (unit 2a), evidencing the 1638 event. Unit 1 may be considered the colluvial wedge related to 1638. Previous events are discussed in the text.

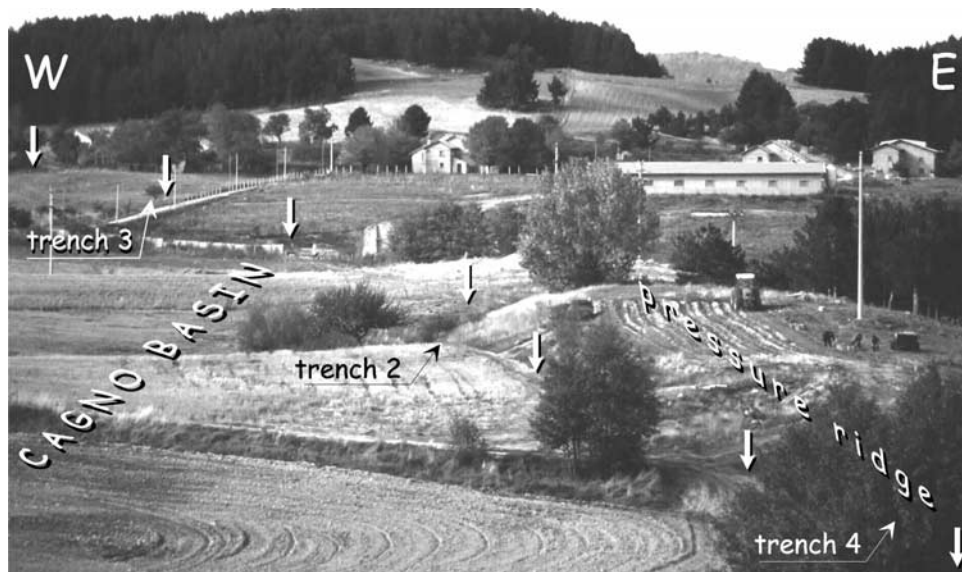


**Figure 10.** Panoramic view of northern Cagno basin. White arrows indicate the fault scarp trace. Sites of trenches 2–4 are also reported. The Cagno basin is dammed by the “pressure ridge,” which grew along the fault.

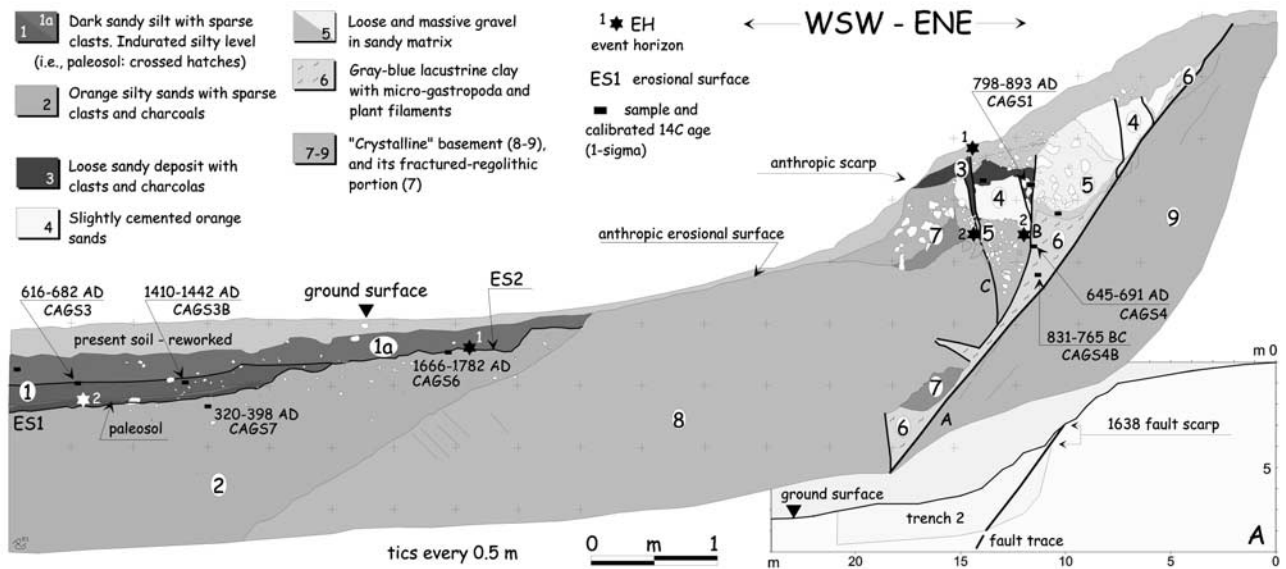


**Figure 11.** Sketch of northern wall of trench 2. Inset A is the topographical section across the fault scarp, and it shows the net scarplet due to the 1638 event. Note the “flower structure” feature in the fault zone, possibly related to the horizontal component of the motion.

rently controlled by the owner of the field). Marsh deposits are represented by unit 1a, which is transgressive over both unit 1 and 2 during 1666–1782 A.D. (sample CAGS6). Thus, we propose that this event is the 1638 one. A penultimate event might have occurred prior to the deposition of an other damming/marsh episode (unit 1), being also responsible for the opening of cracks along faults B and C filled by unit 3. Its age must be post 320–398 A.D. (CAGS7, charcoal under the paleosol developed on unit 2), around 612–686 A.D., 645–691 A.D., and before 798–893 A.D. (respectively CAGS3, reworked charcoal in the transgressive marsh deposit and CAGS4 and CAGS1, charcoals trapped at the bottom and top of the open chasm along fault B) (EH2).

[47] Finally, the fabric and geometry of units 4–6 account for other displacement events, although their timing is not defined. The elevation of unit 6 is at least 4 m higher than very similar lacustrine grayish blue clays, which outcrop below unit 1a along the walls of the drainage canal of the present basin. This observation may provide a rough slip rate of 1.4 mm/yr during the past 3 millennia, although the horizontal component of the fault might have produced an apparent uplift of unit 6, trapped in a upward-dragged lithon.

### 5.3. Trench 3

[48] This trench was excavated in the northern part of the Cagno basin, across a smooth scarp within a cultivated field (site 3 in Figure 4 and Figures 10 and 12). The crystalline ridge characterizing the central and southern part of the basin is no longer present in this sector, which is also characterized by a gently bending of the fault westward. Unfortunately, the agricultural works reworked the upper part of the natural deposits, obliterating the most recent deformation history.

[49] The trench walls show a branched fault system, dipping 60°SW, with several subvertical-to-reverse splays, affecting almost all the exposed deposits with a dominant

normal component. Crystalline rocks outcrop in the footwall (unit 13) and, similarly to trench 2, a squeezed wedge of gray lacustrine clay (Figure 13) (unit 12, see unit 6 of trench 2) is trapped along fault B. On the other hand, unit 2 is the anthropic filling of a tensional fissure opened along fault B (enlarged by the ancient villagers in order to build an underground drainage canal), composed by big boulders (bottom) and stratified sands and gravels (top). Unit 2 contains a rounded ( $\phi$  10 cm) piece of glass, which probably belonged to a oil lantern felt in the open chasm.

[50] Units outcropping in the hangingwall are made by alternating sands–gravel–silts alluvial deposits (units 3–11), with a wedge of lacustrine clay (unit 12) (same clay trapped along fault B) packed at the bottom of the exposed succession along fault A. In particular, units 8 and 4 are brownish sandy silts, rich in organic material, very similar to the present marsh deposits that we observed in the neighboring drainage canals. Unit 4 thickens toward west (depocenter of the basin), as shown by a pit excavated 3 m away from the trench (see log of pit 4 in Figure 13). Units 5 and 6 are the filling of an alluvial canal carved in the underlying deposits. Finally, unit 1 at the top is a reworked gray coarse sand, related to the extensive agricultural work of the 1950s, which contributed to the remodeling of the fault scarp.

[51] The age of the whole succession is constrained by seven  $^{14}\text{C}$  ages of charcoals sampled within the trench. The older one is in unit 8 (1892–1603 B.C.) (sample CAG01), while the entire alluvial–marsh succession (units 7–4) was deposited between 1500 and 1100 B.C. (see Table 3). The glass found inside unit 2 has been dated to the 17th to early 18th century, on the basis of its manufacturing (C. Gueragni Nolli, personal communication, 2001).

[52] Apart from units 1 and 2, all the outcropping succession is faulted. The last event, sealed by units 1 and 2, should be responsible for the opening of the tensional fissure along the fault B; the chasm is filled by unit 2, which



**Figure 12.** View looking north along LF scarp in the northernmost Cagno basin, where we opened trench 3. The scarp is highly degraded and reworked by the intense agricultural works. This site is far from the basin-saddle, and trench 3 provided information on older deposits with respect to trenches 2, 4.

is an anthropic deposit, probably dated to the 17th to early 18th century (age of the glass). We relate this event to the 1638 earthquake (EH1).

[53] According to the available ages, there are more than 2500 years of sedimentary hiatus before the 17th century A.D. However, this trench provides information on older events of surface faulting; starting from the oldest, a paleoevent is evidenced by the faulting of unit 9 (fault C) (EH4), sealed by unit 8. The latter could be interpreted as a

marsh deposit filling the basin dammed by the coseismic footwall uplift. EH4 could be thus tentatively dated quite before 1892–1603 B.C., the age of a charcoal (CAG01) collected inside unit 8. The marsh deposits piled up in the hangingwall (unit 8), due to the subsequent erosion of the pond threshold (i.e., the fault scarp), have been successively eroded by an alluvial canal (ES1) and replaced by unit 7 (fine gravels and coarse sands), the age of which is 1515–1427 B.C., as suggested by a charcoal date (CAG17). Unit 7 is then faulted by faults D and E, while unit 6, another marsh deposit, marks a new damming of the canal, which is filled then by unit 5 and mantled by other marsh deposits (unit 4). Assuming again a tectonic control of the basin threshold, we can tentatively date this further paleoevent around 1261–1186 B.C. (sample CAG2, a big angular piece of charcoal), age of the canal damming (EH3).

[54] Units 4–9 have been then displaced by a successive event (fault F), which could be either the 1638 or a previous, unknown one (EH2).

**5.4. Trench 4**

[55] Trench 4 is the southernmost one of the Cagno basin (site 4 in Figure 4). It has been excavated within an entrenched valley, very close to the stream bottom. Also in this place the fault scarp has been exploited by the natives in order to build up a small pond (which was dried during trenching). The excavated deposits (see Figure 14) are mainly coarse to fine sands, angular gravels, silty peat and sparse clasts and boulders, besides grayish blue lacustrine

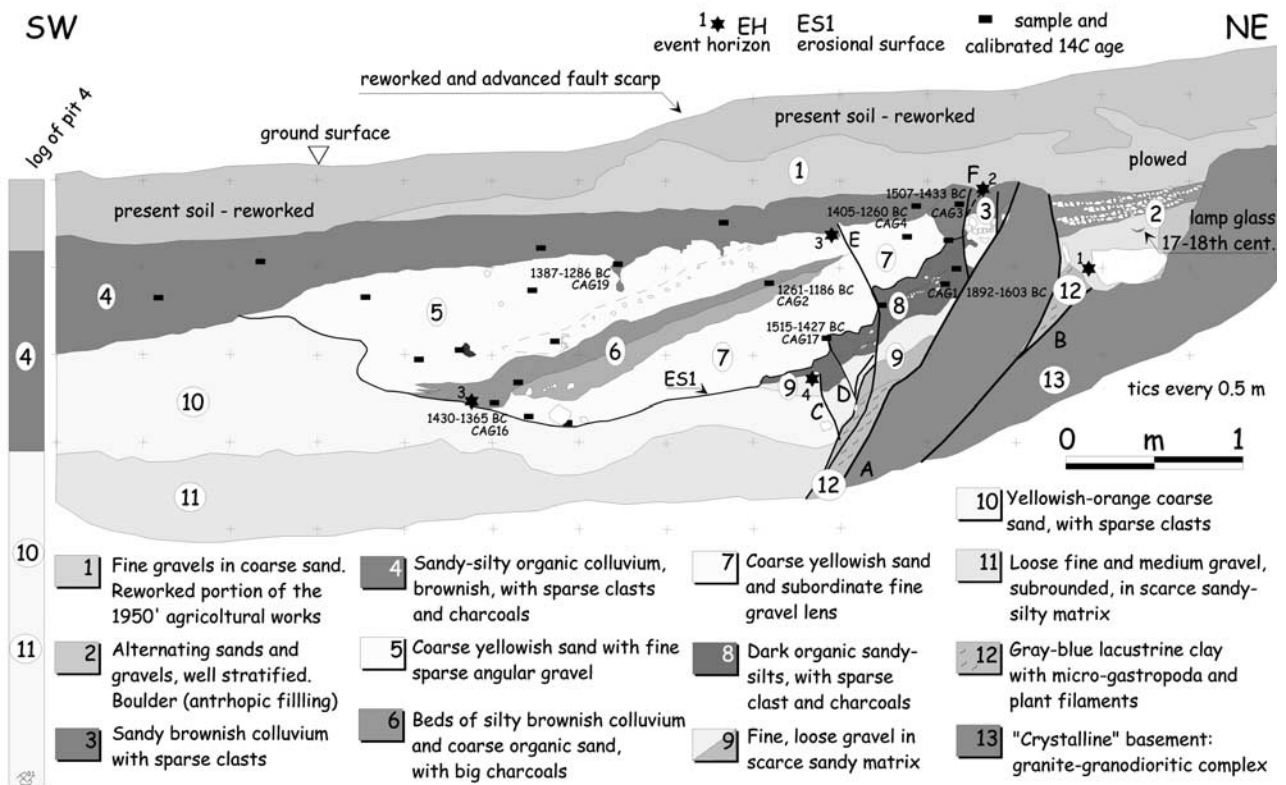


**Figure 13.** Sketch of trench 3, excavated in the northern Cagno basin. The villager exploited the chasm opened in 1638 along fault B for drying up the marsh area. They refilled the open fracture with gravel and boulders (unit 2), where we found an ancient piece of a lamp glass.

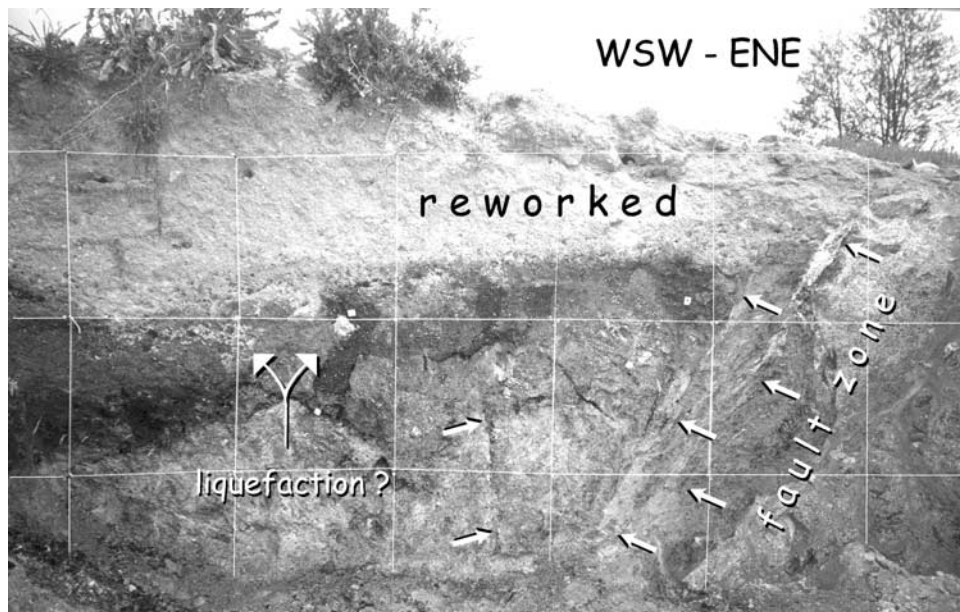


**Figure 14.** View of northern wall of trench 4. The structural complexity of the fault zone (white arrows) is increased by possible liquefaction phenomena, which disturbed and further deformed the beds.

clays squeezed along the fault plane. The alluvial–colluvial succession (hangingwall) is faulted and dragged over a whitish, altered granite mass (footwall). The intense deformation and distorted structure of the deposits made very difficult the identification and definition of the depositional units, which seems also to have experienced liquefaction processes and gravitational sliding during the shaking. Moreover, all the upper part of the trench wall shows reworked material (both plowed and bulldozed) related to the pond works.

[56] The  $^{14}\text{C}$  ages of this complex succession range between 792 and 545 B.C. (sample CAGC1, unit 6) and 776–900 A.D. (sample CAGC4, unit 3), the age of 1182–1299 A.D. (CAGC2) belonging to a tree root underexcavating units 1–3 (Figure 15).

[57] All the outcropping deposits are faulted and only the plowed level seals the displaced units. We deduce that the event that caused the faulting and the deformation of the entire sequence is also responsible for the deposition of unit 1. The latter, due to its geometry and internal structure (loose chaotic mixture of sand and softy pebbles of unit 5), might be, in fact, interpreted as a sandblow intruded from unit 5 in units 2 and 3. We relate this ultimate event to 1638 (EH1).

[58] A penultimate event (EH2) is suggested by the presence of unit 3, which is a marsh deposit (very dark brownish silty sand, rich in organic material) abruptly developed over a coarse sandy deposit (unit 5) hosting big boulders fallen from the footwall. The marsh is interpreted as the consequence of the coseismic damming of the basin (footwall uplift) that occurred slightly before 776–900 A.D. (CAGC4). This event is also evidenced by fault C, which is sealed by unit 3 (although fault C might also be related to a previous event, discussed forward).

[59] The marsh was then gradually filled by sandy deposits and, at least since 1182–1299 A.D., the trees of the nearby forest recolonized the area (CAGC2, a big root

remnant, which we believe to have grown after the reclamation/drainage of the marsh (unit 2), thus predating EH1).

[60] Tentatively, a previous event is again suggested by the nature and shape of unit 6, an other dark, rich in organic material silt, which has been dragged upward by faults A, B, and C. Both interpreting it as a marsh deposit due to an other damming event or as a colluvial wedge deposited (faulted at least twice) along the fault scarp, the age of the causative event should be slightly before 792–545 B.C. (CAGC1) (EH3).

## 6. Discussion

[61] The paleoseismological analyses carried out in the trenches show that LF is the causative fault of the 9 June 1638 event. Moreover, its location and characteristics fit exactly with the contemporary descriptions of the surface faulting phenomena that occurred during this earthquake.

[62] Among all the known central southern Apennine active faults [Galadini and Galli, 2000; Cinque et al., 2000], this fault pairs up only with an other fault which was unknown until the 1980,  $M_s = 6.9$  earthquake: the Irpinia fault [Pantosti et al., 1993]. Similarly to the latter, in fact, the LF ruptures in a manner that is at odds with topography, running at high elevation through the granitic massif of Sila and far from fully developed Quaternary basins. Its kinematics, as deduced by field evidence, is mainly normal, but with a not negligible horizontal slip. This oblique component may account for some geomorphic expression (pressure ridge, pushup swell and sag depression) occurring at some releasing and restraining bends (eastern and western, respectively) along the main strike.

[63] Moreover, the young geomorphic expression of the LF would suggest its relatively recent activation within the extensional regime characterizing the Apennine chain and the Calabrian arc. Considering that the stress field in southern Apennine depicts a NE-SW extension [see Montone et

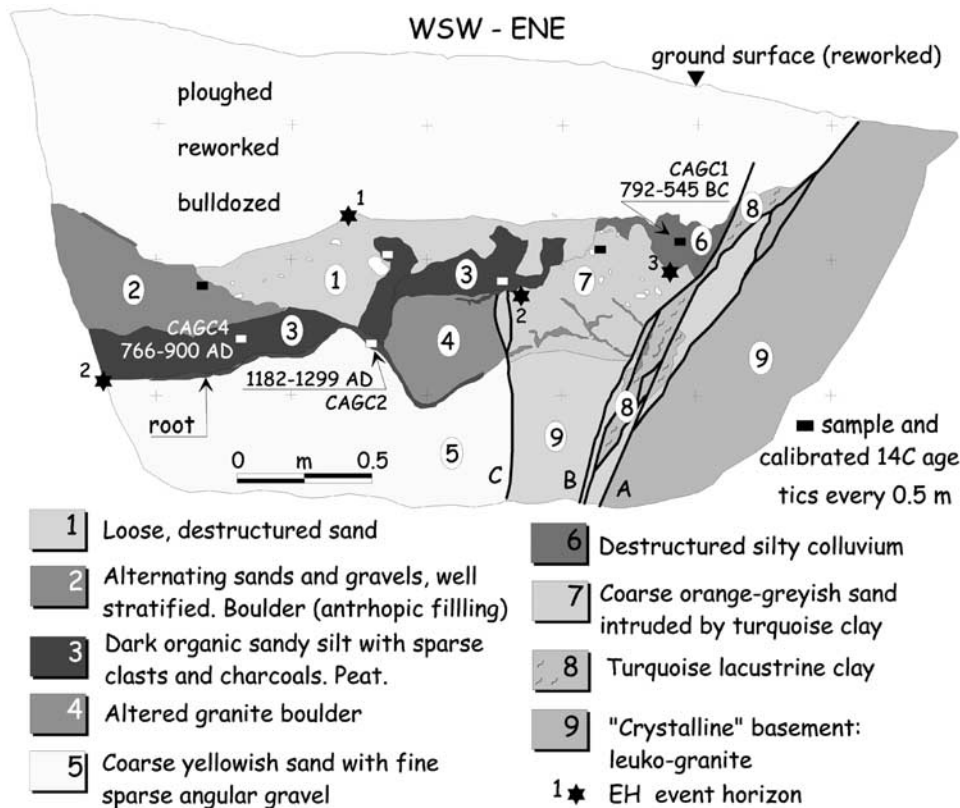


**Figure 15.** Sketch of northern wall of trench 4. Notwithstanding the bulldozing of the entire area (a small pond was created by exploiting the natural fault scarp-barrage), which erased the surficial deposits, 2–3 events are still evidenced by the deformational history of the lacustrine-marsh deposits.

*al.*, 1999, and references therein], the kinematic indication observed along the LF, together with the few available local focal mechanisms (Figure 3), evidences a persisting Apenninic NE-SW extension in northern Calabria. On the other hand, extension dramatically rotates southward to the Catanzaro strait in a NW-SE direction, as evidenced by fault orientation and focal mechanism of southern Calabria [Galli and Bosi, 2002, and references therein].

[64] As for the parameter of the June event, on the basis of the evaluated intensities datapoints (Table 2), we obtained a macroseismic equivalent magnitude (Boxer program) [Gasperini, 1999] of  $M_e = 6.68$  and a fault length of 31 km. Moreover, in order to disassemble the “missing intensities” at the epicenter (due to the aforementioned lack of any villages in the inner Sila massif) we added three fictitious  $I = 11$  MCS datapoints along the LF trace, which yielded quite the same parameters of  $M_e$  (6.74) and fault length (34 km) (Table 1). This trial, based on the observation that  $I = 11$  MCS is commonly reached by villages located close to faults with dimension similar to LF [e.g., Galadini and Galli, 2000; Galli and Bosi, 2002], provides reasonable parameters to the June event, which we included in Table 1.

## 6.1. Seismic Behavior

### 6.1.1. Paleoeearthquakes

[65] Even if discontinuous, the stratigraphic record observed in the trenches shows evidence, through its deformational history, of repeated 1638-like paleoeearthquakes. The ages of paleoeearthquakes recognized in the individual trenches have been correlated assuming that each

time the fault rupture is the same. The ultimate event in all trenches is the 1638 earthquake, its age been constrained between <sup>14</sup>C ages of 1564–1628 and 1666–1782 A.D. and by a glass of the 17th century. The penultimate event occurred in the 7th and 8th century A.D. (our preferred age after <sup>14</sup>C age of 645–691 A.D. and before 798–893 A.D., 776–900 A.D.). This event is well constrained in trench 2 and 4, it is compatible with the data coming from trench 1, whereas it is not seen in trench 3 due to the lack of sediments (Figure 16). Data coming from Trench 1 suggest also an event occurring slightly before or around the 3rd century B.C., while, according to the interpretation made in trench 3, other two probable similar events occurred in the 12th and 21th century B.C., respectively.

### 6.1.2. Recurrence Time

[66] Although the reliability of the oldest age of deformation events may be questionable, we observe a rough elapsed time interval of 800–1000 years between consecutive events. This value could be thus indicative of the return period of the LF.

### 6.1.3. Slip Rates

[67] Although there are no beds to correlate across the main fault, and the horizontal component of motion represents a bias for the in-trench evaluation of the offset, the historical description of the 1638 surface faulting suggests a reliable value (80 cm) [Di Somma, 1641] of the vertical offset per event (sensu “characteristic earthquake”). This offset is similar to that estimated in trench 1 by restoring back the faulted succession and fits, eventually, with the “fresh” step commonly affecting the foot of the LF scarp

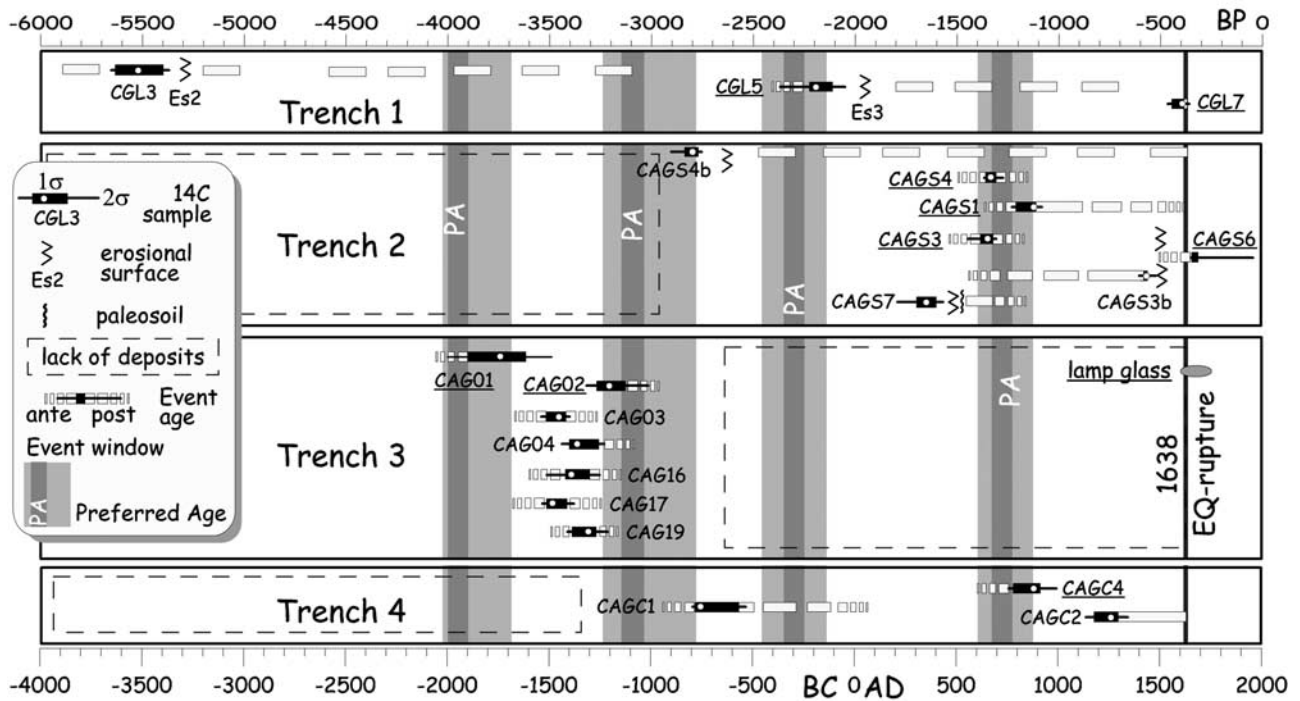


**Figure 16.** Sketch summarizing ages of samples, erosional surfaces, and paleosoils in trenches. Age is shown through both 1- $\sigma$  and 2- $\sigma$  ranges (black box and lines, respectively); underlined samples are those which better constrain the age of paleoearthquakes. Dashed gray boxes indicate whether the paleoearthquake occurred before (leftward/before) or after (rightward/after) the age of the sample (the longer the box, the more uncertain and farther the date of the event is). The width of event window depends mainly by the age range of samples, while preferred age is constrained by the geologic interpretation of trenches.

(Figures 5 and 11a). Considering also the horizontal component (which seems prominent, even if smaller than the vertical one), we hypothesize a net (oblique) surficial offset of 1–1.2 m per event. This value, coupled with the hypothesized recurrence time, gives a slip rate of 1.2 mm/yr, not far from that roughly estimated in trench 2 in the past 3 ka (1.4 mm/yr). Finally, coupling slip per event and fault length we obtain a  $M_o = 6.7$ , which is the same value gathered for Me.

**6.2. Fault Segmentation**

[68] As mentioned before, the LF is not an isolated structure through the Sila Massif. We hypothesize that, through an en echelon right step, its northern continuation is the CLF (5 in Figure 3) (Figure 6), a NNW-SSE system which shares with the LF the same tendency to invert the topography creating ephemeral ponds.

[69] Differently to LF, CLF appears to be seismically quiescent in the last millennium, none of the strong historical earthquakes of the Italian catalogue being consistent with its location. Only the 1184 event (see Figure 1 for its rough epicentral location), which is known to have induced severe damage in the Crati Valley and along the western slope of Sila, could be doubtfully related to this fault.

**6.3. Seismic Hazard Implication**

[70] Seismic hazard studies in Italy [e.g., Lucantoni et al., 2001], together with the proposed Seismic Reclassification of the Italian territory [Working Group, 1999] are currently based on a probabilistic method [Cornell, 1968] which implies the use of a “declustered” catalogue [Camassi and

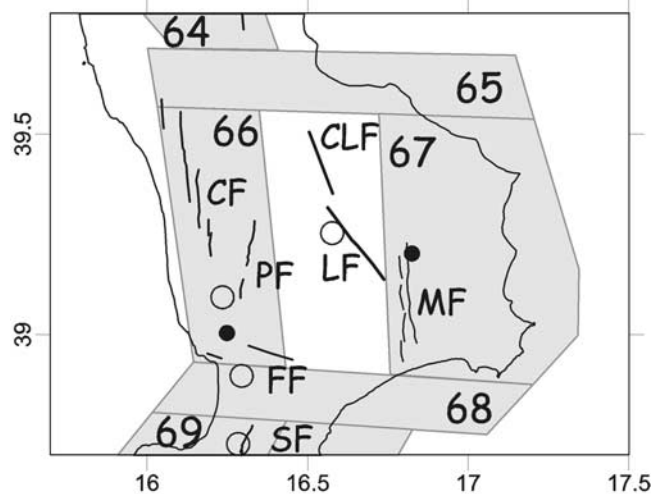


**Figure 17.** Seismogenetic zones of northern Calabria according to Meletti et al. [2000]. Note the “background” area between zones 66 and 67, which should be instead the main seismogenetic zone. Bold lines are LF CLF, Crati faults (CF), Piano Lago–Savuto faults (PF), Feroletto–Santa Eufemia (Lamezia-Catanzaro FF) and Serre fault (SF). Thin lines are the Marchesato fault (MF) [Moretti, 2000]. Filled and empty circles are, the Working Group CPTI [1999] and our epicenters, respectively, for the 1638 March (west) and June (east) events.

Stucchi, 1997] coupled with a seismogenetic zonation of the Italian territory [Meletti *et al.*, 2000, and references herein].

[71] In this framework, the discovery of LF, and its relationships with the neighboring faults and with the historical seismicity provide new important data that radically change both the historical database and the geometry of the seismogenetic zones.

[72] On one hand the epicenter of the June 1638 event is shifted by 15–20 km westward with respect to the macroseismic epicenter (see Figure 1) [Camassi and Stucchi, 1997; Working Group CPTI, 1999]. On the other hand, the discovery of LF, together with CLF, dramatically influences the geometry and the parameter of the some seismogenetic zones of the region [i.e., zone 67 in Meletti *et al.*, 2000] (see Figure 17), which are mainly based on the June 1638 macroseismic epicenter [Camassi and Stucchi, 1997] and on the location of the Marchesato faults (Figures 3 and 17). As mentioned before, the latter were hypothetically considered the causative faults of the June 1638 event [Moretti, 2000], even in the lack of any evidence of Upper Pleistocene–Holocene activity.

[73] According to the present seismogenetic zonation, the LF and its associated earthquakes, together with the CLF, would fall in a “seismic background zone,” whereas zone 67 would miss the most severe (and characterizing in terms of maximum expected magnitude and earthquake recurrence) event within its boundary (Figure 17). Seismic hazard would dramatically change also in the western part of the region, where the 27 March event has now been split into three events ( $M \leq 6.6$ ), which fall in three different zones (66, 68, and 69 in Figure 17).

[74] Concluding, while new parameters should be evaluated for zone 66 and neighbors (Figure 17), a new zone should be drawn between 66 and 67, or new borders should be considered for zone 67, in order to include the Sila seismogenetic area.

[75] Finally, using different hazard methods (i.e., hybrid recurrence model) [Wu *et al.*, 1995], one should be take into account that while the LF ruptured in 1638 (having an apparent return period of about 1 ka), the elapsed time related to the CLF is presently comparable to its possible recurrence time.

#### 6.4. Associated Hydrological Risk

[76] Both LF and CLF pass very close to the masonry/concrete barriers which, respectively, dam the Ampollino and Cecita lakes. The LF capability to produce surface displacement (assumed also for CLF), associated to the high level of shaking related to the “near-field” condition, are factors that would strongly affect the possible collapse of the dams (see surface faulting effects on dams in Seno [1999]). Therefore, considering the capacity of the lakes ( $67 \times 10^6$  and  $121 \times 10^6$  m<sup>3</sup>, respectively), the eventual break of the dams would trigger a hydrological disaster on a vast inhabited area along the valleys below, as far as the alluvial Crati plain (Cecita Lake) and the Ionian coast (Ampollino Lake).

## 7. Conclusions

[77] We took both a historical and geological approach to the revisiting of one of the most catastrophic seismic sequence of Italy.

[78] The analyses of all the available historical sources concerning the 27 March 1638 event allowed us to recognize at least 3 main shocks occurring between the evening of 27 and the day of 28 March. The first and more catastrophic shock hit the area southward of Cosenza, and we tentatively relate this event to the southern continuation of the western Crati Valley fault system (e.g., Piano Lago and Savuto–Decollatura faults) (7 in Figure 3); the second shock hit the western slope of the Serre range, an area characterized by the northern prosecution of the Mesima fault system (9 in Figure 3). The third event struck the western Catanzaro strait, being possibly related to the Santa Eufemia–Feroletto fault (8 in Figure 3). The magnitude of these events is minor of the one reported by Working Group CPTI [1999] ( $M_e = 7$ ), being possibly  $\leq 6.6$ .

[79] As for the June earthquakes, the analyses of the historical sources permitted to split this event into three separated shocks, the most catastrophic being that of 9 June. This sequence affected the eastern slope of Sila, its effects being not negligible until the far NW corner of the massif. The historical description of the surficial breaks allowed us the identification of the causative fault (and of the physic epicenter) running inside the mountainous uninhabited area. This fact implies that, although we reevaluated a maximum MCS intensity of 9.5, the real epicentral intensity ( $I_0$ ) could be higher (i.e., 11 MCS).

[80] This newly identified structure, referred to the LF (6 in Figure 3), is a northwesterly striking, west-dipping normal fault, with horizontal component. The results of the paleoseismological analysis show evidence for a historical event of surface faulting, that we interpreted as the June 1638 one, and for a penultimate event in the 7th and 8th century A.D., not reported by the Italian seismic catalogue. Others paleoearthquakes, although lacking of definitive cross correlation among trenches, seems to be occurred about the 3rd, 12th, and 21th century B.C.

[81] Assuming that we do not miss any event of surface faulting, according to data summarized in Figure 16, we suggest a recurrence period of about 0.8–1 ka for this structure. Slip rate, deduced from individual offset and long-term displacement, was estimated to be in the order of 1.2 mm/yr. The LF continues northward with a right en echelon step in the CLF (5 in Figure 3). The latter, which can be responsible for the uplift of the Pleistocene beds of the paleo-Cecita lake, is characterized by the absence of any historical earthquakes in the past millenia (or, doubtfully, at least since 1184 A.D.). By comparing the recurrence time of LF with other seismogenetic faults of central and southern Apennines (1.4–2 ka) [Pantosti *et al.*, 1993; Galadini and Galli, 2000; Galli and Bosi, 2002], we may tentatively assume that the CLF shares the same seismic behavior too. If this is the case, with such an average time recurrence range (i.e., 1–2 ka), the CLF contains a high potential for producing an earthquake in the near future.

[82] The data presented in this paper imply the necessity to reassess the seismic hazard of the region, the local seismogenetic zones currently mismatching the real epicenters (the June one being shifted westward) and the associated seismogenetic faults (Figure 17).

[83] Finally, the presence of important barrier lakes across LF and CLF are a further element of hydrological risk in case of earthquake. The collapse of the dams of the Ampollino and

Cecita lakes, due to their impressive capacity, would trigger a hydrological disaster in a vast inhabited area downstream both basins.

[84] **Acknowledgments.** We are grateful to Salvatore Loria who allowed trenching in his properties. We are also grateful to Giovanna Chiodo who supported our historical researches and to Antonio Moretti and Ignazio Guerra who provided useful geologic and instrumental data. We also thank Paolo De Martini, Marco Moro, and Daniela Pantosti who strengthened our paleoseismological interpretation within the trenches. Mario Perri dug with consummate skill all trenches. Costanza Gueragni Nolli kindly examined the lamp glass. Criticism of the Associate Editor, of Daniela Pantosti, and of an anonymous referee strongly improved the manuscript. Field survey was performed during 2000–2001. The view and conclusion contained in this paper are those of the authors and should not be interpreted as necessarily representing the official policies, either expressed or implied, of the Italian Government.

## References

- Amato, A., B. Alessandrini, G. B. Cimini, A. Frepoli, and G. Selvaggi, Active and remnant subducted slabs beneath Italy: Evidence from seismic tomography and seismicity, *Ann. Geofis.*, **36**, 201–214, 1993.
- Barchi, M., G. Minelli, and P. Piali, The Crop 03 profile: A synthesis of results on deep structures of the Northern Apennines, *Mem. Soc. Geol. It.*, **52**, 383–405, 1998.
- Bernaudo, F., *Il tremuoto di Calabria. Discorso*, Napoli, 1639.
- Bianchi, P., *Relazione di Paolino Bianchi al segretario di stato sui danni causati dal terremoto delle due Calabrie*, Napoli, 1638.
- Bond, G., W. Showers, M. Cheseby, R. Lotti, P. Almasi, P. deMenocal, P. Priore, H. Cullen, I. Hajdas, and G. Bonani, A pervasive millennial-scale cycle in North Atlantic Holocene and glacial climates, *Science*, **278**, 1257–1266, 1997.
- Boschi, E., E. Guidoboni, G. Ferrari, D. Mariotti, G. Valensise, and P. Gasperini (Eds.), Earthquakes of 27 March and 8 June 1638, in *Catalogue of Strong Italian Earthquakes From 461 BC to 1997*, *Ann. Geofis.*, **43**, 835–841, 2000.
- Bousquet, J. C., La tectonique recent de l'Apennin Calabro-Lucanien dans son cadre geologique et geophysique, *Geol. Rom.*, **12**, 1–103, 1973.
- Camassi, R., and M. Stucchi, NT4.1.1 un catalogo parametrico di terremoti di area italiana al di sopra della soglia del danno, 95 pp., GNDT, Milan, 1997. (Available at <http://emidius.itim.mi.cnr.it>).
- Capecelatro, E., Relazione (breve) al Vicerè del Regno di Napoli duca di Medina di Las Torres fatta consigliere Hettore Capece-Latro, a rivedere i danni nelle provincie di Calabria, cagionati dal terremoto succeduto a 27 di marzo 1638, per applicarci i rimedi necessari, per la sollevazione di quelle Città, Terre, e Castelli, che hanno patito, Napoli, 1640a.
- Capecelatro, E., Danno succeduto per lo terremoto de gli otto del corrente mese di giugno, Appendix in D'Orsi [1640], Napoli, 1640b.
- Capecelatro, E., Relazione al Vicerè del regno di Napoli duca di Medina di Las Torres, de' danni c'han patito l'infrascritte università per cagion de' terremoti il di' 27 di marzo 1638 con nota distinta de' morti, e case cascate nella provincia di calabria ultra, napoli 20 giugno 1638, Appendix in D'Orsi [1640], Napoli, 1640c.
- Chiodo, G., I terremoti calabri del 1638, Relazione finale, Educ. grant EDIS Calabria, 1993.
- Chiodo, G., I. Guerra, and J. Trumper, The 1638 earthquakes, migratory phenomena and geolinguistic consequences in Calabria, *Ann. Geofis.*, **38**, 515–521, 1995.
- Cinque, A., A. Ascione, and C. Caiazzo, Distribuzione spazio-temporale e caratterizzazione della fagliazione quaternaria in Appennino meridionale, in *Le ricerche del GNDT nel campo della pericolosità sismica*, edited by F. Galadini et al., pp. 203–218, CNR-GNDT, Rome, 2000.
- Cinti, F. R., L. Cucci, D. Pantosti, G. D'Addezio, and M. Meghraoui, A major seismogenic fault in a "silent area": The Castrovillari fault (southern Apennines, Italy), *Geophys. Int.*, **130**, 595–605, 1997.
- Compassionevole relazione delli spaventosi terremoti occorsi nella Calabria, & altri luoghi. Col nome delle città, e terre sommerse, e rounate da detti terremoti. Seguiti questo presente anno 1638, alli 27 di marzo, Pietro Nesti, Firenze, 1638.
- Cornell, C. A., Engineering seismic risk analysis, *Bull. Seismol. Soc. Am.*, **58**, 1583–1606, 1968.
- D'Amato, V., Memorie storiche dell'illustrissima, famosissima e fedelissima città di Catanzaro, Napoli, 1670.
- Descriptive relation of the terrible earthquake of Calabria of the 27 March 1638 (in Polish), Varszawa, 1638.
- D'Orsi, L., *I terremoti delle due Calabrie fedelissimamente descritti dal Si. Lutio D'Orsi di Belcastro come testimonio di vedute*, Napoli, 1640.
- Di Somma, A., *Historico racconto dei terremoti della Calabria dell'anno 1638 fin'anno 1641*, Napoli, 1641.
- Dramis, F., and B. Gentili, G. Pambianchi, Geomorphological scheme of the River Trionto basin, in *Symposium on Geomorphology of Active Tectonics Areas*, edited by M. Sorriso Valvo, IGU-COMTAG and CNR, Excursion Guidebook, IRPI, Cosenza, Geodata 39, pp. 63–66, 1990.
- Dreadful newes: or a true relation of the great, violent and late earthquake. Hapned the 27 day of March, stilo romano, last, at Calabria, in the Kingdome of Naples, about the houres of three and foure in the afternoone, tot the over-trow and mine of many Cities, Townes, and Castles, and the death of about fifty thousand persone, edited by I. Okes, for R. Mab, 17 pp., London, 1638.
- Finetti, I., and A. Del Ben, Geophysical study of the Tyrrhenian opening, *Bol. Geofis. Teor. Appl.*, **28**, 75–155, 1986.
- Finetti, I., and C. Morelli, Geophysical exploration of the Mediterranean Sea, *Bol. Geofis. Teor. Appl.*, **15**, 263–344, 1973.
- Galadini, F., and P. Galli, Active tectonics in the central Apennines (Italy): Input data for seismic hazard assessment, *Nat. Hazards*, **22**, 202–223, 2000.
- Galli, P., Active tectonics along the Wadi Araba–Jordan Valley transform fault, *J. Geophys. Res.*, **104**, 2777–2796, 1999.
- Galli, P., and V. Bosi, Paleoseismology along the Cittanova fault: Implications for seismotectonics and earthquake recurrence in Calabria (southern Italy), *J. Geophys. Res.*, **107**(B3), 2044, doi:10.1029/2001JB000234, 2002.
- Galli, P., and F. Galadini, Seismotectonic framework of the 1997–98 Umbria-Marche (Central Italy) earthquakes, *Seismol. Res. Lett.*, **70**, 404–414, 1999.
- Gasperini, P., The Boxer program, 1999. (Available at <http://ibogfs.df.unibo.it/user2/paolo/www/boxer/boxer.html>).
- Ghisetti, F., and L. Vezzani, Different styles of deformation in the Calabrian Arc (Southern Italy): Implication for a seismotectonic zoning, *Tectonophysics*, **25**, 149–165, 1982.
- Giunchi, C., R. Sabadini, E. Boschi, and P. Gasperini, Dynamic models of subduction: Geophysical and geological evidence in the Tyrrhenian Sea, *Geophys. J. Int.*, **126**, 555–578, 1996.
- Gueguen, E., C. Doglioni, and M. Fernandez, Lithospheric bouidange in the western Mediterranean back-arc basins, *Terra Nova*, **9**, 184–187, 1997.
- Henderson, G., Carta Geologica della Calabria alla scala di 1:25.000, sheet 230, CASMEZ, 1973.
- Jacques, E., C. Monaco, P. Tapponnier, T. Tortorici, and T. Winter, Faulting and earthquake triggering during the 1783 Calabria seismic sequence, *Geophys. J. Int.*, **147**, 499–516, 2001.
- Keigwin, L. D., and E. A. Boyle, Detecting Holocene changes in thermohaline circulation, *Proc. Natl. Acad. Sci. U.S.A.*, **97**, 1343–1346, 2000.
- Kircher, A., *Mundus subterraneus in XII libros digestus, Calabria*, Amsterdam, 1665.
- Lucantoni, A., V. Bosi, F. Brammerini, R. De Marco, T. Lo Presti, G. Naso, and F. Sabetta, Seismic risk in Italy, *Ing. Sismica*, **18**, 5–36, 2001.
- Martire, D., *Calabria Sacra e Profana*, manuscript of the 18th century, Bibl. Civ. Cosenza, 1704.
- Matano, F., and S. Di Nocera, Weathering patterns in the Sila massif (northern Calabria, Italy), *Ital. J. Quat. Sci.*, **12**, 141–148, 1999.
- Meletti, C., E. Patacca, and P. Scandone, Construction of a seismotectonic model: The case of Italy, *Pure Appl. Geophys.*, **157**, 11–35, 2000.
- Monachesi, G., and M. Stucchi, DOM 4.1 an intensity database of damaging earthquakes in the Italian area, 1998. (Available at <http://emidius.itim.mi.cnr.it/DOM/home.html>).
- Monaco, C., and L. Tortorici, Active faulting in the Calabrian arc and eastern Sicily, *J. Geodyn.*, **29**, 407–424, 2000.
- Montone, P., A. Amato, and S. Pondrelli, Active stress map of Italy, *J. Geophys. Res.*, **104**, 2595–2610, 1999.
- Moretti, A., Note sull'evoluzione tettono-stratigrafica del Bacino Crotonese dopo la fine del Miocene, *Bol. Soc. Geol. Ital.*, **112**, 845–867, 1993.
- Moretti, A., Il database delle faglie capaci della Calabria, in *Le ricerche del GNDT nel campo della pericolosità sismica (1996–1999)*, edited by F. Galadini et al., pp. 219–226, CNR-Gruppo Nazionale per la Difesa dai Terremoti, Rome, 2000.
- Moretti, A., and I. Guerra, Tettonica dal Messiniano ad oggi in Calabria: Implicazioni sulla geodinamica del sistema Tirreno-Arco Calabro, *Bol. Soc. Geol. Ital.*, **116**, 125–142, 1997.
- Pantosti, D., G. D'Addezio, and F. Cinti, Paleoseismological evidence of repeated large earthquakes along the 1980 Irpinia earthquake fault, *Ann. Geofis.*, **36**, 321–330, 1993.
- Paragallo, G., *Ragionamento intorno alla cagione de' tremuoti*, Ed. Fasulo Geronimo, Napoli, 1689.
- Parker, M., *A True and Terrible Narration of a horrible Earthquake which happened in the Province of Calabria... upon the 27 of March last past according to Foraigne account, and by our English computation the*

- 17... *From pregnant atestation written in English verse by M. Parker. With a ... list of some other Earthquakes and horrible accidents which have heretofore happened in England*, T. Cotes for R. Mabb and F. Grove (Editors), London, 1638.
- Patacca, E., and P. Scandone, Late thrust propagation and sedimentary response in the thrust-belt–foredeep system of the Southern Apennines (Pliocene–Pleistocene) in *Anatomy of an Orogen: The Apennines and Adjacent Mediterranean Basins*, edited by G. B. Vai and I. P. Martini, pp. 401–440, Kluwer Acad., Norwell, Mass., 2001.
- Recupito, G. C., *De novo in universa Calabriae terraemotu congemminatus nuncijs*, Napoli, 1638.
- Regio Ufficio Geologico d'Italia, Geological Map of Italy, sheet 237, scale 1:100,000, Rome, 1895.
- Relazione del terremoto successo nelle province di Calabria di 8 giugno 1638, Biblioteca Apostolica Vaticana, ms. Barberini Latini 4336, 1638.
- Scaccianoce, A., Il terremoto del 9 giugno 1638: analisi delle fonti storiche ed interpretazione sismotettonica, degree thesis, Univ. of Calabria, Cosenza, 1993.
- Seno, T., Report on the surface ruptures of the Taiwan earthquake on Sept. 20, 1999, 1999. (Available as <http://www.eri.u-tokyo.ac.jp/seno/taiwan.report.eng.html>).
- Siani, G., M. Paterne, E. Michel, R. Sulpizio, A. Sbrana, M. Arnold, and G. Haddad, Mediterranean sea surface radiocarbon reservoir age changes since the last glacial maximum, *Science*, 294, 1917–1920, 2001.
- Sorriso-Valvo, M., and C. Tansi, Grandi frane e deformazioni gravitative profonde di versante della Calabria. Note illustrative della carta al 250.000, *Geogr. Fis. Din. Quat.*, 19, 395–408, 1997.
- Stucchi, M., and P. Albini, Quanti terremoti distruttivi abbiamo perso nell'ultimo millennio? Spunti per la definizione di un approccio storico alla valutazione della completezza, in *Le ricerche del GNDT nel campo della pericolosità sismica (1996–1999)*, edited by F. Galadini et al., pp. 333–344, CNR-Gruppo Nazionale per la Difesa dai Terremoti, Rome, 2000.
- Stuiver, M., P. Reimer, E. Bard, W. Beck, G. S. Burr, K. Hughen, B. Kromer, G. McCormac, J. van der Plicht, and M. Spurk, INTCAL98 radiocarbon age calibration, 24,000–0 cal, *Radiocarbon*, 40, 1041–1084, 1998.
- Tortorici, L., C. Monaco, C. Tansi, and O. Cocina, Recent and active tectonics in the Calabrian arc (Southern Italy), *Tectonophysics*, 243, 37–55, 1995.
- Trumbore, S. E., *Radiocarbon Geochronology, Quaternary Geochronology: Methods and Applications*, AGU Ref. Shelf 4, 2000.
- Van Dijk, J. P., and P. J. J. Scheepers, Neotectonic rotations in the Calabrian Arc: Implication for a Pliocene–Recent geodynamic scenario for the Central Mediterranean, *Earth Sci. Rev.*, 39, 207–246, 1995.
- Vera relatione del spaventevole terremoto successo alli 27 di marzo sù le 21 hore, nelle provincie di Calabria Citra, & Ultra, Ludovico Grignani, Roma, 1638.
- Westaway, R., Quaternary uplift of southern Italy, *J. Geophys. Res.*, 98, 21,741–21,772, 1993.
- Working Group, Proposal for the National Seismic Reclassification, *Ing. Sismica*, 1, 5–14, 1999.
- Working Group CPTI, *Catalogo Parametrico Terremoti Italiani*, 92 pp., ING, GNDT, SGA, SSN, Bologna, 1999.
- Wu, S. C., C. A. Cornell, and S. R. Winterstein, A hybrid recurrence model and its implication on seismic hazard, *Bull. Seismol. Soc. Am.*, 85, 1–16, 1995.

---

V. Bosi and P. Galli, Civil Protection Department, Seismic Survey of Italy, Via Curtatone 3, I-00185, Rome, Italy. ([paolo.galli@serviziosismico.it](mailto:paolo.galli@serviziosismico.it))